Structural, electronic, magnetic and optical properties of Ni and Cd based full-Heusler alloys using first principle calculation

Roll: MS191306
Session: 2019-2020

Thesis submitted to the Department of Physics at
Jashore University of Science and Technology
in partial fulfillment of the requirements
for the degree of Masters of Science
in Physics

March 2023

Abstract

The electronic, magnetic and optical properties of Ni and Cd based full-Heusler alloys, Ni_2NbSi, Ni_2ZrGe, Cd_2MnAs and Cd_2MnSb, are studied using the spin polarized full-potential linearized augmented plane wave (FP-LAPW) method based on Density Functional Theory (DFT). The exchange correlation potential PBE-GGA approach, as implemented in the WIEN2k code, is used to investigate band structure, density of states, and optical spectra for these Heusler compounds. The optimized lattice parameters were estimated to be 5.93 Å, 6.13 Å, 6.90 Å and 7.15 Å for Ni_2NbSi, Ni_2ZrGe, Cd_2MnAs and Cd_2MnSb respectively. Our study reveals that the alloys are metallic in nature since both the spin up and spin down states are conducting. The optical performance of the compounds is determined by analyzing real and imaginary dielectric function components, optical absorption, reflectivity and refractivity spectra.

Acknowledgements

Foremost, I want to praise the almighty Allah, who enabled me to continue this work and leading towards the fulfillment of the requirements for the degree of Masters of Science in Physics.

I would like to express my great gratitude to my supervisor Dr. Mohammad Abdur Rashid, for his continuous supervision, constant guidance, enthusiasm, patience and constructive criticisms that provided immense help in preparing this report. I am grateful to him because of the untiring effort and contributions to the development of my work.

My sincere thanks goes to all the faculaty members of the Depertment of physics for their encouragements and insightful comments which led me to prepare for my future career.

My deepest appreciation belongs to my parents for their love, unconditional supporting and prayers in all steps in my life. Their love and encouragement always gives me mental support to continue my study smoothly.

Contents

Structural, electronic, magnetic and optical properties of Ni and Cd based full-Heusler alloys using first principle calculation

List of Figures

List of Tables

Structural, electronic, magnetic and optical properties of Ni and Cd based full-Heusler alloys using first principle calculation

Chapter 1

Introduction

In recent years, Heusler alloys have received more attention due to their fascinating physical features [1–4], especially the half-metallic (HM) character, which was first specified by de Groot et al in 1983 [5]. whose majority-spin band is metalic while the minority-spin band is semiconducting with an energy gap at the Fermi level (E_{F}). Half-metallic (HM) ferromagnets have gathered great attention from scientific researchers due to potential applications in spintronic devices, such as the magnetic sensor, the tunnel junction, the spin valve as well as the primary materials in the electrode [6, 7]. The presence of peculiarity makes such materials to maximize the efficiency of spintronic devices [8]. Heusler alloys have a special importance due to their higher Curie temperatures (T_{c}) and tunable electronic structure [9–11]. The magnetic Heusler alloys have become increasingly important because of their multifunctional properties which render them useful in different domains from spintronics to magnetic shape-memory and magnetocaloric technologies [12–22]. The strong magnetoelastic interactions in the magnetic Heusler alloys are responsible for novel functional properties such as the magnetic-shape memory and magnetocaloric effects (MSME & MCE) [12,14,15]. Heusler alloys are of significant interest among scientific community due to the number of the distinguished properties such as shape memory effect, effects of super elasticity and superplasticity, giant magnetocaloric effect, giant magnetoresistance and magnetostrain, etc. This attempts the advantage to a new generation of devices that integrate standard microelectronics with spin-dependent effects, such as nonvolatile magnetic random access memories and magnetic sensors [23].

The two main types of Heusler alloys are full-Heusler and half-Heusler alloys. Half-metallic Heusler alloys that are used in spintronic device applications [24]. Half metallic magnetic materials with 100% spin polarization (SP) at the interface of the valence and conduction bands have received a lot of attention. The general formula for ternary Heusler compounds is X_2YZ, where X and Y are transition metals and Z is a main group element. The full-Heusler compound consists of four fcc sublattices with base as: A (0, 0, 0), B (0.25, 0.25, 0.25), C (0.5, 0.5, 0.5) and D (0.75, 0.75, 0.75) [25]. In structures such as $AlCu_2Mn$ with space group (225, $FM\bar{3}m$), the X atoms occupy A and C sites, the Y atom in the B site, and the Z atom occupy the D site. While, in $CuHg_2Ti$ with space group (216, $F4\bar{3}m$), A and B sites are occupied by X atoms while C and D sites are occupied by Y and Z respectively. These configurations mainly are affected by valence electrons of X and Y atoms [26–28].

In this report, we present an attempt of density functional theory (DFT) study for Ni and Cd based alloys, Ni_2NbSi, Ni_2ZrGe, Cd_2MnAs and Cd_2MnSb. In condensed matter physics, quantum chemistry, and material science, density functional theory based electronic structure calculations are becoming more and more common. Density functional theory is by far the most widely used approach for electronic structure calculations nowadays. It is usually called first principle method or ab initio method, because it allows people to determine many properties of a condensed matter system by just giving some basic structural information without any adjustable parameter [29]. Another important element of DFT is the precise approximation for the exchange-correlation functional, which comes from the Kohn-Sham approach [30].

The report is organized as follows: in chapter one, we illustrate the general introduction of Heusler alloys. We describe the fundamentals of quantum mechanics in chapter two, including Schrödinger's groundbreaking equations, the time-independent Schrödinger equation, the wave function, atoms and molecules, and the many-body system. The fundamental density functional theory is covered in chapter three. It contains electron density, Thomas-Fermi direct approximation, Hohenberg-Kohn theorems, Kohn-Sham equations, the exchange-correlation functional, local density approximation (LDA), and generalized-gradient approximation (GGA). We discuss our entire calculation method and structure, band structure, density of state (DOS), partial density of state (PDOS), and optical properties of these materials in chapter four. The summary of this functioning system is covered in Chapter five.

Chapter 2

Basic Quantum Mechanics

Quantum mechanics is a useful tool for understanding the electronic structure of chemical compounds and the processes, thermodynamics, and kinetics of chemical reactions at a theoretical level [31]. It can be thought of roughly as the study of physics on very small length scales, although there are certain macroscopic systems it directly applies to. On the scale of atoms and subatomic particles, it explains how matter behaves and interacts with energy. This chapter goes through basic concepts and expressions, as well as the most basic forms that are applicable to many-body systems. In quantum physics, particles display wavelike properties, and the Schrödinger equation, a particular wave equation, governs the behavior of these waves. The Schrödinger equation is different in a few ways from the other wave equations. Despite these modifications, all of our typical techniques for solving a wave equation and processing the resulting solutions still hold.

2.1 Schrödinger's groundbreaking equation

The principle of density functional theory are conveniently expounded by making reference to conventional wave function theory. Any problem in the electronic structure of matter is covered by Schrödinger's equation including the time. In most cases, however, one is concerned with atoms and molecules without time-dependent interactions, so we may focus on the time-independent Schrödinger's equation [32]. In 1926, Erwin Schrödinger attempted to characterize's matter wave's by using de Broglie's connections to describe hypothetical plane waves, resulting in the most generic form of the famous equation named after him, the

time-dependent Schrödinger equation [33].

$$i\hbar\frac{\partial}{\partial t}\Psi(\vec{r},t) = \hat{H}\psi(\vec{r},t) \tag{2.1}$$

Where, $\hat{H}$ is the hamiltonian operator, $\hbar$ is the dirac constant and Ψ is the wave function. It is often impracticable to use a complete relativistic formulation of the formula; therefore Schrödinger himself postulated a non-relativistic approximation which is nowadays often used, especially in quantum chemistry. Using the Hamiltonian for a single particle

$$\hat{H} = \hat{T} + \hat{V} = -\frac{\hbar^2}{2m}\vec{\nabla}^2 + V(\vec{r},t) \tag{2.2}$$

leads to the (non-relativistic) time-dependent single-particle Schrödinger equation

$$i\hbar\frac{\partial}{\partial t}\Psi(\vec{r},t) = [-\frac{\hbar^2}{2m}\vec{\nabla}^2 + V(\vec{r},t)]\Psi(\vec{r},t) \tag{2.3}$$

The Hamiltonian for N particles in three dimensions is

$$\hat{H} = \sum_{i=1}^{N}\frac{\hat{p}_i^2}{2m_i} + V(\vec{r}_1,\vec{r}_2,...\vec{r}_N,t) = -\frac{\hbar^2}{2}\sum_{i=1}^{N}\frac{1}{m_i} + V(\vec{r}_1,\vec{r}_2,....\vec{r}_N,t) \tag{2.4}$$

The corresponding Schrödinger equation reads

$$i\hbar\frac{\partial}{\partial t}\Psi(\vec{r}_1,\vec{r}_2,....\vec{r}_N,t) = [-\frac{\hbar^2}{2}\sum_{i=1}^{N}\frac{1}{m_i}\nabla_i^2 + V(\vec{r}_1,\vec{r}_2,....\vec{r}_N,t)]\Psi(\vec{r}_1,\vec{r}_2,....\vec{r}_N,t) \tag{2.5}$$

2.2 Time-independent Schrödinger equation

Special cases are the solutions of the time-independent Schrödinger equation, where the Hamiltonian itself has no time-dependency (which implies a time-independent potential V $(\vec{r_1},\vec{r_2},...,\vec{r_N}\,)$ and the solutions therefore describe standing waves which are called stationary states or orbitals). The time-independent Schrödinger equation is not only easier to treat, but the knowledge of its solutions also provides crucial insight to handle the corresponding time-dependent equation. The time-independent equation (2.5) is obtained by the approach of separation of variables, i.e. the spatial part of the wave function is separated from the

temporal part via. [34]

$$\Psi(\vec{r_1}, \vec{r_2}, ..., \vec{r_N}, t) = \psi(\vec{r_1}, \vec{r_2}, ..., \vec{r_N})\tau(t) = \psi\vec{r_1}, \vec{r_2}, ..., r_N)e^{\frac{iEt}{\hbar}} \tag{2.6}$$

Furthermore, the l.h.s. of the equation reduces to the energy eigenvalue of the Hamiltonian multiplied by the wave function, leading to the general eigenvalue equation

$$E\psi(\vec{r_1}, \vec{r_2}, ..., \vec{r_N}) = \hat{H}\psi(\vec{r_1}, \vec{r_2}, ..., \vec{r_N}) \tag{2.7}$$

Again, using the many-body Hamiltonian, the Schrödinger equation becomes

$$E\psi(\vec{r_1}, \vec{r_2}, ..., \vec{r_N}) = [-\frac{\hbar^2}{2}\sum_{i=1}^{N}\frac{1}{m_i}\nabla_i^2 + V(\vec{r}_1, \vec{r}_2, ...\vec{r}_N)]\psi(\vec{r}_1, \vec{r}_2, ...\vec{r}_N) \tag{2.8}$$

2.3 The wave function

The wave function ψ has no direct physical meaning. The wave function $\psi(r, t)$ describes the position of a particle with respect to time. It can be considered as probability amplitude. $|\psi|^2$ is proportional to the probability of finding a particle at a particular time. It is the probability density [35, 36]

$$|\psi|^2 = |\psi^*\psi|^2 \tag{2.9}$$

The wave function ψ must be finite everywhere. If ψ is infinite for a par- ticular point, it mean an infinite large probability of finding the particles at that point. This would violates the uncertainty principle. It must be single valued. If ψ has more than one value at any point, it mean more than one value of probability of finding the particle at that point which is obviously ridiculous. The wave function must be continuous and have a continuous first derivative everywhere and its must be normalizable. For the sake of simplicity the discussion is restricted to the time-independent wave function. A question always arising with physical quantities is about possible interpretations as well as observations. The Born probability interpretation of the wave function, which is a major principle of the Copenhagen interpretation of quantum mechanics, provides a physical interpretation for the square of the wave function as a probability density [37, 38]

$$P = |\psi(\vec{r_1}, \vec{r_2}, ..., \vec{r_N}|^2 d\vec{r_1} d\vec{r_2} .... d\vec{r_N} \tag{2.10}$$

Equation (2.10) describes the probability that particles 1, 2, ..., N are located simultaneously in the corresponding volume element $d\vec{r_1}\ d\vec{r_2}\ ....d\vec{r_N}$ [39]. What happens if the positions of two particles are exchanged, must be considered as well. Following merely logical reasoning, the overall probability density cannot depend on such an exchange, i.e.

$$|\psi(\vec{r_1}, \vec{r_2}, ..., \vec{r_i}, \vec{r_j}, ..., \vec{r_N})|^2 = |\psi(\vec{r_1}, \vec{r_2}, ..., \vec{r_j}, \vec{r_i}, ..., \vec{r_N})|^2 \tag{2.11}$$

There are only two possibilities for the behavior of the wave function during a particle exchange. The first one is a symmetrical wave function, which does not change due to such an exchange. This corresponds to bosons (particles with integer or zero spin). The other possibility is an anti-symmetrical wave function, where an exchange of two particles causes a sign change, which corresponds to fermions (particles which half-integer spin) [40, 41]. In this text only electrons are from interest, which are fermions. The anti-symmetric fermion wave function leads to the Pauli principle, which states that no two electrons can occupy the same state, whereas state means the orbital and spin parts of the wave function (the term spin coordinates will be discussed later in more detail). The antisymmetry principle can be seen as the quantum-mechanical formalization of Pauli's theoretical ideas in the description of spectra (e.g. alkaline doublets) [42].

Another consequence of the probability interpretation is the normalization of the wave function. If equation (2.10) describes the probability of finding a particle in a volume element, setting the full range of coordinates as volume element must result in a probability of one, i.e. all particles must be found somewhere in space. This corresponds to the normalization condition for the wave function.

$$\int d\hat{r_1} \int d\hat{r_2} ... \int d\hat{r_N} |\psi(\vec{r_1}, \vec{r_2}, ..., \vec{r_N}|^2 = 1 \tag{2.12}$$

Equation (2.12) also gives insight on the requirements a wave function must fulfill in order to be physical acceptable. Wave functions must be continuous over the full spatial range and square-integratable [43]. Calculating the expectation values of operators with a wave function also provides the expectation value of the relevant observable for that wave function [44].

For an observable $O(\vec{r_1}, \vec{r_2}, ..., \vec{r_N})$, this can generally be written as

$$O = \langle O \rangle = \int d\vec{r_1} \int d\vec{r_2} ... \int d\vec{r_N} \psi^*(\vec{r_1}, \vec{r_2}, ..., \vec{r_N}) \hat{O} \psi(\vec{r_1}, \vec{r_2}, ..., \vec{r_N}) \tag{2.13}$$

2.4 Atoms and molecules

Charged particles are present in all atomic and molecular systems. The Schrödinger equation for a single electron, in which the electron moves in a Coulomb potential.

$$i\hbar \frac{\partial}{\partial t} \psi(\vec{r}) = [-\frac{\hbar^2}{2m} \vec{\nabla}^2 - \frac{e^2}{4\pi\epsilon_0} \frac{1}{|\vec{r}|}] \psi(\vec{r}) \tag{2.14}$$

The so-called atomic units are introduced at this stage for future use for the purpose of simplicity. That is, the electron mass m_e, the electron charge e, the reduced Planck constant (Dirac constant), $\hbar$ and the vacuum permittivity factor $4\pi\epsilon_0$ are all equal to one [45].
The Schrödinger equation for the single electron simplifies to

$$E\psi(\vec{r}) = [-\frac{1}{2} \nabla^2 - \frac{1}{|\vec{r}|}] \psi(\bar{r}) \tag{2.15}$$

The Schrödinger equation can be solved analytically in this way. Although the Schrödinger equation will soon be analytically accessible for the description of matter, including atoms. The use of (2.8) allows the development of a generalized many-body Schrödinger equation for a system made up of N electrons and M nuclei ,where external magnetic and electric fields are neglected.

$$E_i \psi_i(\vec{r_1}\vec{r_2}...\vec{r_N}; \vec{R_1}\vec{R_2}...\vec{R_N}) = \hat{H} \psi(\vec{r_1}\vec{r_2}...\vec{r_N}; \vec{R_1}\vec{R_2}...\vec{R_N}) \tag{2.16}$$

Equation (2.16) does not seem overly complicated on the first look, but an examination of the corresponding molecular Hamiltonian

$$\hat{H} = -\frac{\hbar^2}{2m_e} \sum_{i=1}^{N} \nabla_i^2 - \frac{\hbar^2}{2M_k} \sum_{k=1}^{M} \nabla_k^2 - \sum_{i=1}^{N} \sum_{k=1}^{M} \frac{Z_k e^2}{r_{ik}} + \frac{1}{2} \sum_{i=1}^{N} \sum_{j>i}^{N} \frac{e^2}{r_{ij}} + \frac{1}{2} \sum_{k=1}^{M} \sum_{l>k}^{M} \frac{Z_k Z_l}{R_{kl}} \tag{2.17}$$

reveals the real complexity of the equation.

In equation (2.17), M_k represents the nuclear mass in atomic units (i.e. in units of the electron mass), Z_k and Z_l represent the atomic numbers, and $r_{ij} = |\vec{r_i} - \vec{r_j}|, r_{ik} = |r_i - \vec{R_k}|$ and $R_{kl} = |\vec{R_k} - \vec{R_l}|$ represent the distances between electron-electron, electron-nucleus and nucleus-nucleus respectively. A term-by-term interpretation of the right hand side in (2.17) reveals that the first two terms correspond to the kinetic energies of the electrons and nuclei. The latter three terms denote the potential part of the Hamiltonian in terms of electrostatic particle-particle interactions. This is reflected by the corresponding signs, where the negative sign denotes an attractive potential between electrons and nuclei, whereas the positive signs denote repulsive potentials between electrons and electrons as well as the nuclei among themselves [46].

2.5 The Many-Body System and Born-Oppenheimer (BO) Approximation

The Born-Oppenheimer approximation is one of the basic concepts underlying the description of the quantum states of molecules. This approximation makes it possible to separate the motion of the nuclei and the motion of the electrons. In this discussion nuclear refers to the atomic nuclei as parts of molecules not to the internal structure of the nucleus. The Born-Oppenheimer approximation neglects the motion of the atomic nuclei when describing the electrons in a molecule. The physical basis for the Born-Oppenheimer approximation is the fact that the mass of an atomic nucleus in a molecule is much larger than the mass of an electron (more than 1000 times). Because of this difference, the nuclei move much more slowly than the electrons. In addition, due to their opposite charges, there is a mutual attractive force of acting on an atomic nucleus and an electron. This force causes both particles to be accelerated. Since the magnitude of the acceleration is inversely proportional to the mass. The acceleration of the electrons is large and the acceleration of the atomic nuclei is small; the difference is a factor of more than 1000.

As a consequence, the general Hamiltonian is replaced by the so-called electronic Hamiltonian from equation (2.17)

$$\hat{H} = -\frac{\hbar^2}{2m_e}\sum_{i=1}^{N}\nabla_i^2 - \sum_{i=1}^{N}\sum_{k=1}^{M}\frac{Z_k e^2}{r_{ik}} + \frac{1}{2}\sum_{i=1}^{N}\sum_{j>i}^{N}\frac{e^2}{r_{ij}} \tag{2.18}$$

or in terms of operators

$$\hat{H_{el}} = \hat{T} + \hat{U} + \hat{V} = \hat{T} + \hat{V_{tot}} \tag{2.19}$$

Especially for problems of molecular physics and quantum chemistry, the electronic Schrödinger equation is of major interest. But despite all simplifications a simple look at equations (2.16) to (2.19) indicates that there are still a few more crucial points left to deal with until a useful solution can be obtained. Inspection of equations (2.18) and (2.19) shows that the kinetic energy term depend on the nuclear coordinates R_{kl} , or in other words, it is only a function of the electron number. Also the electron-electron repulsion $\hat{\mathrm{U}}$ is the same for every system with only Coulomb interactions. Therefore the only part of the electronic Hamiltonian which depends on the atomic molecular system is the external potential $\hat{V}$ caused by the nucleus-electron repulsion. Subsequently this also means that $\hat{T}$ and $\hat{U}$ only need the electron number N as input and will therefore be denoted as 'universal', whereas $\hat{V}$ is system-dependent. The expectation value of $\hat{V}$ is also often denoted as the external potential V_{ext} , which is consistent as long as there are no external magnetic or electrical fields [44]. As soon as the external potential is known, the next step is the determination of the wave functions ψ_i which contain all possible information about the system. As simple as that sounds, the exact knowledge of the external potential is not possible for most natural systems, i.e. in similarity to classical mechanics, the largest system which can be solved analytically is a two body system, which corresponds to a hydrogen atom. Using all approximations introduced up to now it is possible to calculate a problem similar to H_2^+, a single ionized hydrogen molecule. To get results for larger systems, further approximations have to be made.

2.6 The Hartree-Fock approach

In order to find a suitable strategy to approximate the analytically not accessible solutions of many-body problems, a very useful tool is variational calculus, similar to the least-action principle of classical mechanics. By the use of variational calculus, the ground state wave function ψ_0, which corresponds to the lowest energy of the system E_0 , can be approached. A useful literature source for the principles of variational calculus has been provided by T. Flieÿbach [47]. Hence, for now only the electronic Schrödinger equation is of interest, therefore in the following sections we set $\hat{H} \equiv \hat{H_e}l$,$E \equiv E_e l$, and so on. Observables in

quantum mechanics are calculated as the expectation values of operators [48,49]. The energy as observable corresponds to the Hamilton operator, therefore the energy corresponding to a general Hamiltonian can be calculated as

$$E = \langle \hat{H} \rangle = \int d\vec{r_1} \int d\vec{r_2} ... \int d\vec{r_N} \psi^*(\vec{r_1}, \vec{r_2}, ..., \vec{r_N}) \hat{H} \psi(\vec{r_1}, \vec{r_2}, ..., \vec{r_N}) \tag{2.20}$$

The Hartree-Fock technique is based on the principle that the energy obtained by any (normalized) trial wave function other than the actual ground state wave function is always an upper bound, i.e. higher than the actual ground state energy. If the trial function happens to be the desired ground state wave function, the energies are equal

$$E_{trial} \geq E_0 \tag{2.21}$$

with

$$E_{trial} = \int d\vec{r_1} \int d\vec{r_2} ... \int d\vec{r_N} \psi^*_{trial}(\vec{r_1}, \vec{r_2}, ..., \vec{r_N}) \hat{H} \psi_{trial}(\vec{r_1}, \vec{r_2}, ..., \vec{r_N}) \tag{2.22}$$

and

$$E_0 = \int d\vec{r_1} \int d\vec{r_2} ... \int d\vec{r_N} \psi^*_0(\vec{r_1}, \vec{r_2}, ..., \vec{r_N}) \hat{H} \psi_0(\vec{r_1}, \vec{r_2}, ..., \vec{r_N}) \tag{2.23}$$

The expressions above are usually inconvenient to handle. For the sake of a compact notation, in the following the braket notation of Dirac is introduced. For a detailed description of this notation, the reader is referred to the original publication [50].
In that notation, equations (2.21) to (2.23) are expressed as

$$\langle \psi_{trial} | \hat{H} | \psi_{trial} = E_{trial} \geq E_0 = \langle \psi_0 | \hat{H} | \psi_0 \tag{2.24}$$

Proof: [11] The eigenfunctions ψ_i of the Hamiltonian $\hat{H}$ (each corresponding to an energy eigenvalue E_i form a complete basis set, therefore any normalized trial wave function ψ_{trial} can be expressed as linear combination of those eigenfunctions.

$$\psi_{trial} = \sum_i \lambda_i \psi_i \tag{2.25}$$

The assumption is made that the eigenfunctions are orthogonal and normalized. Hence it is requested that the trial wave function is normalized, it follows that

$$\langle\psi_{trial}|\psi_{trial}\rangle = 1 = \langle\sum_i \lambda_i\psi_i|\sum_j \lambda_j\psi_j\rangle = \sum_i\sum_j \lambda_i^*\lambda_j\langle\psi_i|\psi_j\rangle = \sum_j |\lambda_j|^2 \tag{2.26}$$

On the other hand, following (2.25) and (2.27)

$$E_{trial} = \langle\psi_{trial}|\hat{H}|\psi_{trial}\rangle = \langle\sum_i \lambda_i\psi_i|\hat{H}|\sum_j \lambda_j\psi_j\rangle = \sum_j E_j|\lambda_j|^2 \tag{2.27}$$

Together with the fact that the ground state energy E_0 is per definition the lowest possible energy, and therefore has the smallest eigenvalue ($E_0 \leq E_i$), it is found that

$$E_{trial} = \sum_j E_j|\lambda_j|^2 \geq E_0\sum_j |\lambda_j|^2 \tag{2.28}$$

what resembles equation (2.24). Equations (2.20) to (2.28) also include that a search for the minimal energy value while applied on all allowed N-electron wave-functions will always provide the ground-state wave function (or wave functions, in case of a degenerate ground state where more than one wave function provides the minimum energy). The mathematical framework used above, i.e.rules which assign numerical values to functions, so called functionals, is also one of the main concepts in density functional theory. A function gets a numerical input and generates a numerical output whereas a functional gets a function as input and generates a numerical output [51]. Expressed in terms of functional calculus, where $\psi \to N$ addresses all allowed N-electron wave functions, this means [39]

$$E_0 = \min_{\psi\to N} E[\psi] = \min_{\psi\to N}\langle\psi|\hat{H}|\psi\rangle = \min_{\psi\to N}\langle\psi|\hat{T}+\hat{V}+\hat{U}|\psi\rangle \tag{2.29}$$

Due to the vast number of alternative wave functions on the one hand and processing power and time constraints on the other, this search is essentially unfeasible for N-electron systems. Restriction of the search to a smaller subset of potential wave functions, as in the Hartree-Fock approximation, is conceivable.

2.7 Slater-determination

A slater determinant is a formula in quantum mechanics that describes the wave function of a multi-fermionic system. It satisfies anti-symmetry criteria, and thus the Pauli principle, by changing sign when two electrons are exchanged (or other fermions). Only a small fraction of all potential fermionic wave functions can be expressed as a single slater determinant, but because of their simplicity, they are an important and useful subset. In the Hartree-Fock approach, the search is restricted to approximations of the N-electron wave function by an antisymmetric product of N (normal- ized) one electron wave-functions, the so called spin-orbitals $\chi_i(\vec{x}_i)$ A wave function of this type is called Slater-determinant, and reads [52, 53].

$$\Psi_0 \approx \phi_{SD} = (N!)^{-\frac{1}{2}} \begin{vmatrix} X_1(\vec{x}_1) & X_2(\vec{x}_1) & \cdots & X_N(\vec{x}_1) \\ X_1(\vec{x}_2) & X_2(\vec{x}_2) & \cdots & X_N(\vec{x}_2) \\ \vdots & \vdots & \ddots & \vdots \\ X_1(\vec{x}_N) & X_2(\vec{x}_N) & \cdots & X_N(\vec{x}_N) \end{vmatrix} \tag{2.30}$$

It is important to notice that the spin-orbitals $\chi_i(\vec{x}_i)$ are not only depending on spatial coordinates but also on a spin coordinate which is introduced by a spin function, $\vec{x}_i = \vec{r}_i, s$
A detailed discussions of the spin orbitals and their (necessary) properties is omitted in this text, a detailed treatise is provided in the books by Szabo and Holthausen [52]. As spin orbitals e.g. hydrogen-type orbitals (for atomic calculations) and linear combinations of them are used [54].
Returning to the variational principle and equation (2.29), the ground state energy approximated by a single slater determinant becomes

$$E_0 = \min_{\phi_{SD} \to N} E[\phi_{SD}] = \min_{\phi_{SD} \to N} \langle \phi_{SD} | \hat{H} | \phi_{SD} \rangle = \min_{\phi_{SD} \to N} \langle \phi_{SD} | \hat{T} + \hat{V} + \hat{U} | \phi_{SD} \rangle \tag{2.31}$$

A general expression for the Hartree-Fock Energy is obtained by usage of the Slater determinant as a trial function.

$$E_{HF} = \langle \phi_{SD} | \hat{H} | \phi_{SD} \rangle = \langle \phi_{SD} | \hat{T} + \hat{V} + \hat{U} | \phi_{SD} \rangle \tag{2.32}$$

For the sake of brevity, a detailed derivation of the final expression for the Hartree-Fock energy is omitted. It is a straightforward calculation found for example in the Book by

Schwabl [55]. The final expression for the Hartree- Fock energy contains three major parts [52]

$$E_{HF} = \langle \phi_{SD} | \hat{H} | \phi_{SD} \rangle = \sum_{i}^{N} (i|\hat{h}|i) + \frac{1}{2} \sum_{i}^{N} \sum_{j}^{N} [(ii|jj) - (ij|ji)] \tag{2.33}$$

with

$$(i|\hat{h_i}|i) = \int X_i^*(\vec{x}_i)[-\frac{1}{2}\vec{\nabla}_i^2 - \sum_{k=1}^{M} \frac{Z_k}{r_{ik}}]X_i(\vec{x}_i)d\vec{x}_i \tag{2.34}$$

$$(ii|jj) = \iint |X_i(\vec{x}_i)|^2 \frac{1}{r_{ij}} |X_j(\vec{x}_j)|^2 d\vec{x}_i d\vec{x}_j, \tag{2.35}$$

$$(ii|jj) = \iint |X_i(\vec{x}_i) X_j^*(\vec{x}_j) \frac{1}{r_{ij}} X_j(\vec{x}_j) X_i^*(\vec{x}_i) d\vec{x}_i d\vec{x}_j \tag{2.36}$$

The first term corresponds to the kinetic energy and the nucleus-electron interactions, $\hat{h}$ denoting the single particle contribution of the Hamiltonian,whereas the latter two terms correspond to electron-electron interactions. They are called Coulomb and exchange integral, respectively [52,53]. Examination of equations (2.33) to (2.36) furthermore reveals, that the Hartree-Fock energy can be expressed as a functional of the spin orbitals $E_{HF} = E[\{\chi_i\}]$ Thus,variation of the spin orbitals leads to the minimum energy [52]. An important point is that the spin orbitals remain orthonormal during minimization. This restriction is accomplished by the introduction of Lagrangian multipliers λ_i the resulting equations, which represent the Hartree-Fock equations. For a detailed derivation, the reader is referred to the book by Szabo and Ostlund [52, 53, 56].

Finally, one arrives at

$$\hat{f} X_i = \lambda_i X_i \qquad i = 1, 2, ..., N \tag{2.37}$$

with

$$\hat{f_i} = -\frac{1}{2}\vec{\nabla}_i^2 - \sum_{k=1}^{M} \frac{Z_k}{r_{ik}} + \sum_{i}^{N} [\hat{J}_j(\vec{x}_i) - \hat{K}_j(\vec{x}_i)] = \hat{h_i} + \hat{V}^{HF}(i) \tag{2.38}$$

the Fock operator for the $i \rightarrow$th electron.In similarity to (2.33) to (2.36), the first two terms represent the kinetic and potential energy due to nucleus-electron interaction, collected in the core Hamiltonian $\hat{h}_i$ operators,whereas the latter terms are sums over the Coulomb operator $\hat{J}_j$ and the exchange operators $\hat{K}_j$ with the other j electrons, which form the Hartree-Fock potential $\hat{V}^{HF}$. There the major approximation of Hartree-Fock can be seen. The two

electron repulsion operator from the original Hamiltonian is exchanged by a one-electron operator $\hat{V}^{HF}$ which describes the repulsion in average [52].

2.8 Limitations and failings of the Hartree-Fock approach

The number of electrons in an atom or a molecule might be even or odd. The compound is in a singlet state if the number of electrons is even and they are all in double occupied spatial orbitals, ϕ_i. Closed-shell systems are what they are called. Open-shell systems are compounds with an odd number of electrons and compounds with single occupied orbitals, i.e. species with a triplet or higher ground state. These two sorts of systems relate to two different Hartree-Fock techniques. The restricted HF technique (RHF) considers all electrons to be coupled in orbitals,whereas the unconstrained HF method (UHF) removes this restriction entirely. Open-shell systems may alternatively be described using an RHF method, in which only the single occupied orbitals are eliminated, resulting in a limited open-shell HF (ROHF), which is more realistic but also more difficult and hence less popular than UHF [57]. Closed-shell systems, on the other hand, need an unlimited approach to get good outcomes. For example, a system that places both electrons in the same spatial orbital cannot properly describe the dissociation of H_2 (i.e. the behavior at high internuclear distances), because one electron must be positioned at one hydrogen atom. As a result, in HF calculations, technique selection is always crucial [58].

Kohn states several $M = p^5$ with $3 \leq p \leq 10$ parameters for an output with adequate accuracy in the investigations of theH_2 system [59]. For a system with $N = 100$ electrons, the number of parameters rises to

$$M = p^{3N} = 3^{300} to 10^{300} \approx 10^{150} to 10^{300} \tag{2.39}$$

According to equation (2.40), energy reduction would have to be done in a space with at least 10^{150}dimensions, which is well above current computer capabilities. As a result, HF methods are limited to situations involving a modest number of electrons ($N \approx 10$). This barrier is commonly referred to as the exponential wall because of the exponential component in equation (2.33) [59]. Because a multi-electrode wave function cannot be fully characterized by a single Slater determinant, the energy determined by HF calculations is always greater

than the precise ground state energy. The Hartree-Fock limit is the highest precise energy available using HF methods [57].

2.9 Correlation Energy

The exact wave funtion for a system of many interacting electrons is never a single determinant or a simple combination of a few determinants,however.the calculation of the error in energy, called correlation energy, here defined to be negative,

$$E_{corr}^{HF} = E - E_{HF} \tag{2.40}$$

is a major problem in many-body theory on which there has been a vast amonut of work and much progress has been made. The mean-field approximation utilized in the HF method contributes the most to the correlation energy. That is one electron moves in the average field of the others, a method that ignores the fundamental connection between electron motions. To better grasp what this implies, consider electron repulsion at short distances, which is not addressed by a mean-field technique like the Hartree-Fock method [57]. Correlation energy tends to remain constant for atomic and molecular can changes that conserve the numbers and types of chemical bonds,but it can change drastically and become determinative when bonds change.its magnitude can vary from 20 or 30 to thousands of kilocalories per mole, from a few hundredths of an atomic unit on exchange energies are an order of magnitude or more bigger,even if the self-exchange term is omitted.

Chapter 3

Density Functional Theory(DFT)

The most popular technique for simulating periodic systems in quantum mechanics during the past 30 years has been density functional theory. It has recently been adopted by quantum chemists as well, and it is currently extensively utilized for simulating the energy surfaces of molecules. In this lecture, we highlight the characteristics that have led to the widespread adoption of density functional theory and introduce the fundamental ideas that underlie it. The performance of functional family families is evaluated, and recent advancements in exchange correlation functionals are introduced [60]. Density Functional Theory (DFT) is a computational quantum mechanical modeling method used in physics, chemistry and material science to investigate the electronic structure of many body system in particular atoms, molecules and the condensed phases. Using this theory, the properties of many electron system can be determined by using functional, function of another function, which in this case is the spatially dependences electron density. Hence the name density functional theory comes from the use of functions of the electron density. The success of modern DFT method is based on the suggestion by Kohn and Sham 1965 that the electron kinetic energy should be calculated from an auxiliary set of orbitals used for representing the electron density [61].

The main idea of DFT is to describe a many-body interacting system via its particle density and not via its many-body wavefunction. Its significance is to reduce the 3N degrees of freedom of the N-body system to only three spatial coordinates through its particle density. Its basis is the well known Hohenberg-Kohn (HK), which claims that all properties of

a system can be considered to be unique functionals of its ground state density. Together with the Born-Oppenheimer (BO) approximation and Kohn-Sham (KS) ansatz, practical accurate DFT calculations have been made possible via approximations for the so called exchange-correlation (XC) potential, which describes the effects of the Pauli principle and the Coulomb potential beyond a pure electrostatic interaction of the electrons. Since it is impossible to calculate the exact (XC) potential (by solving the many-body problem exactly), a common approximation is the so called local density approximation (LDA) which locally substitutes the XC energy density of an inhomogeneous system by that of a homogeneous electron gas evaluated at the local density. In many cases the results of DFT calculations for condensed matter systems agreed quite satisfactorily with experimental data, especially with better approximations for the XC energy functional since the 1990s. Also, the computational costs were relatively low compared to traditional ways which were based on the complicated many-electron wave function, such as Hartree-Fock theory and its descendants. Despite the improvements in DFT, there are still difficulties in using DFT to properly describe intermolecular interactions; charge transfer excitations; transition states, global potential energy surfaces and some other strongly correlated systems; and in calculations of the band gap of some semiconductors [62].

3.1 A new base variable-the electron density

A general statement concerning the computation of observables has been presented in section 2.3 about the wave function ψ. This section is about a quantity that is computed in a similar manner. The electron density (for N electrons) as the fundamental variable of density functional theory is stated as [57, 63]

$$n(\vec{r}) = N \sum_{s_1} \int d\vec{x}_2 ... \int d\vec{x}_N \Psi^*(\vec{x}_1, \vec{x}_2, ..., \vec{x}_N)\Psi(\vec{x}_1, \vec{x}_2, ..., \vec{x}_N). \tag{3.1}$$

It's worth noting that the notation in (3.1) takes into account a wave function with spin and spatial coordinates. In more detail, the integral in the equation represents the chance of finding a certain electron with any spin in the volume element $d\vec{r}_1$. Because electrons are indistinguishable, N times the integral equals the likelihood of finding any electron there. Other electrons with arbitrary spin and spatial coordinates are represented by the wave function $\psi(\vec{x_1}, \vec{x_2}, ..., \vec{x_N})$ [57].

If the spin coordinates are not taken into account, the electron density can be described as a quantifiable observable that is simply reliant on spatial coordinates [63].

$$n(\vec{r}) = N \int d\vec{r}_2 ... \int d\vec{r}_N \Psi^*(\vec{r}_1, \vec{r}_2, ..., \vec{r}_N)\Psi(\vec{x}_1, \vec{r}_2, ..., \vec{r}_N). \tag{3.2}$$

which can e.g. be determined by X-ray diffraction [57]. Before providing a method that uses electron density as a variable, make sure it has all of the relevant system information. That is to say, it must include information on the electron number N as well as the external potential, which is denoted by $\hat{V}$ [57].
Integrating the electron density across the geographical variables yields the total number of electrons [57].

$$N = \int d\vec{r} n(\vec{r}). \tag{3.3}$$

3.2 Thomas-Fermi theory

The predecessor to DFT was the Thomas-Fermi (TF) model proposed by Thomas and Fermi in 1927. The basic idea of the theory is to find the energy of electrons in a spatially uniform potential as a function of density. Then one uses this function of the density locally even when the electrons are in the presence of an external potential. The problem of electrons interacting by a Coulomb interaction in a uniform background (jellium) is unfortunately not possible to solve exactly, except in the limit of high density. It was solved approximately with the Hartree-Fock approximation. The strategy here will be to use the results of the Hartree-Fock approximation to obtain an approximate account of any term in Schrödinger's equation that cannot automatically be expressed in terms of density. In this method, they used the electron density $n(r)$ as the basic variable instead of the wavefunction. The total energy of a system in an external potential $V_{ext}(r)$ is written as a functional of the electron density $n(r)$ as:

$$E_{TF}[n(\vec{r})] = A_1 \int n(\vec{r})^{\frac{5}{3}} d\vec{r} + \int n(\vec{r}) V_{ext}(\vec{r}) d\vec{r} + \frac{1}{2} \iint \frac{n(\vec{r}) n(\vec{r\prime})}{|\vec{r} - \vec{r\prime}|} d\vec{r} d\vec{r\prime} \tag{3.4}$$

where the first term is the kinetic energy of the non-interacting electrons in a homogeneous electron gas (HEG) with $A_1 = \frac{3}{10}(3\pi^2)^{\frac{2}{3}}$ in atomic units . The kinetic energy density of a HEG is obtained by adding up all of the free-electron energy state $\varepsilon k = \frac{k^2}{2}$ up to the Fermi

wave vector $k_F = [3\pi^2 n(\vec{r})]^{\frac{1}{2}}$ as:

$$t_0[n(\vec{r})] = \frac{2}{(2\pi)^3}\int_0^{k_F}\frac{k^2}{2}4\pi k^2 dk = A_1 n(\vec{r})^{\frac{5}{3}} \tag{3.5}$$

The second term is the classical electrostatic energy of the nucleus-electron Coulomb interaction. The third term is the classical electrostatic Hartree energy approximated by the classical Coulomb repulsion between electrons. In the original TF method, the exchange and correlation among electrons was neglected.

In 1930, Dirac extended the Thomas-Fermi method by R adding a local exchange term $A_2\int n(\vec{r})^{\frac{3}{4}}d\vec{r}$ to Eq.(3.1) with $A_2 = -\frac{3}{4}(\frac{3}{\pi})^{\frac{1}{3}}$ which leads Eq.(3.1) to

$$E_{TFD}[n(\vec{r})] = A_1\int n(\vec{r})^{\frac{5}{3}}d\vec{r} + \int n(\vec{r})V_{ext}(\vec{r})d\vec{r} + \frac{1}{2}\iint\frac{n(\vec{r})n(\vec{r\prime})}{|\vec{r}-\vec{r\prime}|}d\vec{r}d\vec{r\prime} + A_2\int n(\vec{r})^{\frac{4}{3}}d\vec{r} \tag{3.6}$$

The ground state density and energy can be obtained by minimizing the Thomas-Fermi-Dirac equation (3.3) subject to conservation of the total number (N) of electrons. By using the technique of Lagrange multipliers, the solution can be found in the stationary condition:

$$\delta\{E_{TED}[n(\vec{r})] - \mu(\int n(\vec{r}) - N)\} = 0 \tag{3.7}$$

where μ is a constant known as a Lagrange multiplier, whose physical mean- ing is the chemical potential (or Fermi energy at T = 0 K). Eq.(3.4) leads to the Thomas-Fermi-Dirac equation,

$$\frac{5}{3}A_1\int n(\vec{r})^{\frac{2}{3}} + V_{ext}(\vec{r}) + \int\frac{n(\vec{r\prime})}{|\vec{r}-\vec{r\prime}|}d\vec{r\prime} + \frac{4}{3}A_2 n(\vec{r})^{\frac{1}{3}} - \mu = 0 \tag{3.8}$$

This can be solved immediately to provide the density of the ground state. The approximations utilized in the Thomas-Fermi type approach are so rudimentary that the theory has numerous flaws. The most fundamental flaw is that the theory fails to account for atom-to-atom bonding, preventing molecules and solids from forming. Although it is insufficient to represent electrons in matter, the concept of using electron density as the primary variable demonstrates how DFT works. Thomas-Fermi theory smooths out the charge distribution, because it has no way to know that electrons arrange themselves into separate shells. Thomas-Fermi-Dirac is even less physical; it predicts that at some finite radius the charge distribution drops instantaneously to zero. There have been attempts to develop improved

theories of this type by bringing in dependence upon gradients of the charge distribution. The original Thomas-Fermi theory is most accurate for nearly uniform charge distributions, so it is natural to work out the corrections that would occur for an electron gas in a linearly varying potential, a quadratically varying potential, and so on, using these results to construct an expansion in terms of gra- dients of the density. However, none of the theories of this type has gained wide usage.

3.2.1 Advantage of Thomas-Fermi model

Thomas-Fermi model over other model are, it,s simplicity, clarity, and validity over a wide range of densities and temperature. In Thomas-Fermi model, from density we calculated the kinetic energy approximation term. The kinetic energy expression of Thomas-Fermi theory is also used as a component in more sophisticated density approximation to the kinetic energy within modern orbital free density functional theory.

3.2.2 Limitation of Thomas-Fermi model

Thomas-Fermi model accuracy is limited because the resulting expression for the kinetic energy is only approximate, and because the method does not attempt to represent the exchange energy of an atom as a conclusion of the pauli exclusion principle. This model can not describe the exact external potential term. So this model, is not much important for quantitative predictions in atomic or molecular or solid-state physics.

3.3 The Hohenberg-Kohn (HK) Theorems

DFT was proven to be an exact theory of many body systems by Hohenberg and Kohn in 1964. It applies not only to condensed-matter systems of electrons with fixed nuclei, but also more generally to any system of interacting particles in an external potential $V_{ext}(\vec{r})$. The theory is based upon two theorems. The basic lemma of Hohenberg-Kohn states that not only $n(\vec{r})$ is a functional of $V(\vec{r})$ but that also $V(\vec{r})$ is up to a constant determined by $n(\vec{r})$ uniquely. Following the original approach of Hohenberg and Kohn accompanied by their proof via reductio absurdum, the discussion in this theorems is restricted to non degenerate ground states. This restriction nevertheless does not affect the presented proof for the second theorem and can be lifted as well as for the first theorem.

3.3.1 The HK theorem-I

It states that the external potential $V(\vec{r})$ is a functional of the electrons density $n(\vec{r})$ and, up to an unimportant constant, uniquely determined by it. It is assumed that there exist two external potential $V(\vec{r})$ and $V\prime(\vec{r})$ which differ by more than just a trival constant. Furthermore the assumption is made, that both potentials gives rise to the same electron density $n(\vec{r})$. Clearly arising from the nature of $\vec{V}$ in that case there have to be two different Hamiltonians $\hat{H}$ and $\hat{H}\prime$. Further more Ψ and $\Psi\prime$ have to be different Schrödinger equations. Finally also the energy $\hat{E}$ and $\hat{E}\prime$ associated with the particular wave function differ. It also describe the ground state particle density $n(\vec{r})$ of a system of interacting particles in an external potential $V_{ext}(\vec{r})$ uniquely determines the external potential $V_{ext}(\vec{r})$, except for a constant. Thus the ground state particle density determines the full Hamiltonian, except for a constant shift of the energy. In principle, all the states including ground and excited states of the many-body wavefuntions can be calculated. This means that the ground particles density uniquely determines all properties of the system completely.

3.3.2 Proof of the HK theorem-I

For simplicity, here I only consider the case that the ground state of the system is non degenerate. It can be proven that the theorem is also valid for systems with degenerate ground states. The proof is based on minimum energy principle. Suppose there are two different external potentials $V_{ext}(\vec{r})$ and $V\prime_{ext}(\vec{r})$ which differ by more than a constant and lead to the same ground state density $n_0(\vec{r})$. The two external potentials would give two different Hamiltonians, $\hat{H}$ and $\hat{H}\prime$ which have the same ground state density $V_{ext}(\vec{r})$ but would have different ground state wavefunctions, Ψ and $\Psi\prime$, with $\hat{H}\Psi = E_0\Psi$ and $\hat{H}\prime\Psi\prime = E_0\prime\Psi\prime$. Since $\Psi\prime$ is not the ground state of $\hat{H}$, it follows that

$$\begin{aligned} E_0 &< \langle\Psi\prime|\hat{H}|\Psi\prime\rangle \\ &< \langle\Psi\prime|\hat{H}\prime|\Psi\prime\rangle + \langle\Psi\prime|\hat{H} - \hat{H}\prime|\Psi\prime\rangle \\ &< E_0\prime + \int n_0(\vec{r})[Vext(r) - V\prime_{ext}(r)]dr \end{aligned} \tag{3.9}$$

Similarly

$$\begin{aligned} E_0\prime &< \langle\Psi|\hat{H}\prime|\Psi\rangle \\ &< \langle\Psi|\hat{H}|\Psi\rangle + \langle\Psi|\hat{H}\prime - \hat{H}|\Psi\rangle \end{aligned} \tag{3.10}$$

$$< E_0 + \int n_0(\vec{r})[Vext\prime(\vec{r}) - V_{ext}(\vec{r})]dr$$

Adding Eq. (3.9) and (3.10) lead to the contradiction

$$E_0 + E_0\prime < E_0 + E_0\prime \tag{3.11}$$

Hence, no two different external potentials $V_{ext}(\vec{r})$ can give rise to the same ground state density $n_0(\vec{r})$, i.e., the ground state density determines the external potential $V_{ext}(\vec{r})$, except for a constant. That is to say, there is a one-to-one mapping between the ground state density $n_0(\vec{r})$ and the external potential $V_{ext}(\vec{r})$, although the exact formula is unknown.

3.3.3 HK theorem-II

It states that the ground state energy can be derived from the electron density by the use of variational principle. The electron density, which provides a minimum of the ground state energy, is therefore the exact ground state density. Orginally the second theorem has been proved by variational principle, the proof subsequently provided a different one, namely the so called Constrained-Search approach, introduced by Levy and Lieb. There exists a universal funtional $F[n(\vec{r})]$ of the density, independent of the external potential $V_{ext}(\vec{r})$, such that the global minimum value of the energy funtional $E[n(\vec{r})] \equiv \int n(\vec{r})V_{ext}(\vec{r})dr + F[n(\vec{r})]$ is the exact ground state energy of the system and the exact ground state density $n_0(\vec{r})$ miniminizes this funtional. Thus the exact ground state energy and density are fully determined by the funtional $E[n(\vec{r})]$.

3.3.4 Proof of the HK theorem-II

The universal functional $F[n(\vec{r})]$ can be written as

$$F[n(\vec{r})] \equiv T[n(\vec{r})] + E_{int}[n(\vec{r})] \tag{3.12}$$

where $T[n(\vec{r})]$ is the kinetic energy and $Eint[n(\vec{r})]$ is the interaction energy of the particles. According to variational principle, for any wave function $\Psi\prime$, the energy functional $E[\Psi\prime]$:

$$E[\Psi\prime] = \langle\Psi\prime|\hat{T} + \hat{V}_{int} + \hat{V}_{ext}|\Psi\prime\rangle \tag{3.13}$$

has its global minimum value only when $\Psi\prime$ is the ground state wave function Ψ_0, with the constraint that the total number of the particles is conserved. According to HK theorem

I, $\Psi\prime$ must correspond to a ground state with particle density $n\prime(\vec{r})$ and external potential $V\prime_{ext}(\vec{r})$, then $E[\Psi\prime]$ is a functional of $n\prime(\vec{r})$ According to variational principle:

$$\begin{aligned} E[\Psi\prime] &\equiv \langle \Psi\prime | \hat{T} + \hat{V}_{int} + \hat{V}_{ext} | \Psi\prime \rangle \\ &= E[n\prime(\mathbf{r})] \\ &= \int n\prime(\mathbf{r}) V\prime_{ext}(\mathbf{r}) d\mathbf{r} + F[n\prime(\mathbf{r})] \\ &> E[\Psi_0] \\ &= \int n_0(\mathbf{r}) d(\mathbf{r}) + F[n_0(\mathbf{r})] = E[n_0(\mathbf{r})] \end{aligned} \tag{3.14}$$

Thus the energy functional $E[n(r)] \equiv \int n(r) V_{ext}(r) dr + F[n(r)]$ evaluated for the correct ground state density $n_0(r)$ is indeed lower than the value of this functional for any other density $n(\vec{r})$. Therefore by minimizing the total energy functional of the system with respect to variations in the density $n(\vec{r})$, one would find the exact ground state density and energy [62].

3.3.5 Advantage of Hohenberg-Kohn theorems

Hohenberg-Kohn theorems gives the relations between density and potential using variational principle. And the ground state energy determine for only one density. That density is ground state density. If the density is more than one which density give the minimum energy that density is ground state density. In most of today's applications of DFT, only one direction of the Hohenberg–Kohn theorem is used, to find the ground state density for a given system described by an external potential. For the other direction, the inverse problem, it is a priori not clear if even a potential exists that leads to a given density through the solution of the Schrödinger equation, whether for the interacting or non-interacting system, the problem of v-representability. Specific examples of v-representable densities as well as non-v-representable densities have been identified. So the Hohenberg-Kohn theorems must be v-representable. We calculated all electronic properties from density.

3.3.6 Limitation of Hohenberg-Kohn theorems

Hohenberg-Kohn theorems can not described the non classical term. It can not perfectly described the functional term. If the density is not v-representable, this theorems is not valid.

3.4 The Kohn-Sham equations

Kohn and Sham introduced an orbital approach for evaluating $F_{ni}[n]$ in 1965, which was an important step toward quantitative modeling of electronic structure. In other words, in order to evaluate the kinetic energy of N non interacting particles given only their density distribution $n(r)$, they simply found the corresponding potential, called $v_{eff}(r)$, and used the Schrödinger equation.

$$(-\frac{\hbar^2}{2M}\nabla^2 + v_{eff}(r))\psi_i(r) = \epsilon_i\psi_i(r) \tag{3.15}$$

Such that $n(r) = \sum_{i=1}^{N} |\psi(r)|^2$ the states ψ_i here are ordered so that the energies ϵ_i are non decreasing, and the spin index is included in i. If the ϵ_N is degenerate with ϵ_{N+1}(and also at finite temperatures),fractional occupations f_i are to be used $n(r) = \sum_{i=1}^{\infty} f_i|\psi(r)|^2$, but if only spin degeneracy is involved, the result for the density is not affected. The kinetic energy is then given by,$F_{ni} = \sum_{i=1}^{N} |\langle\psi_i|\hat{t}|\psi_i\rangle = \sum_{i=1}^{N} \epsilon_i - \int drn(r)v_{eff}(r)$ where $\hat{t}_i$ is the kinetic energy operator for the ith electron ($\hat{T} = \sum_i \hat{t}_i$).

In practice, it is the external potential of a given system which is known, not the density distribution or the effective potential. One may find the effective potential by taking a functional derivative of the three-term expression for $F_{HK}[n]$, and rearranging the terms:

$$v_{eff}(r) = v(r) - e\varphi(r) + v_{xc}(r) \tag{3.16}$$

where we have used Equation for both the interacting and noninter- acting system. The electrostatic potential is here

$$\varphi(r) = -e\int dr\prime\frac{n(r\prime)}{|r - r\prime|} \tag{3.17}$$

And the exchange-correlation potential is defined as

$$v_{xc}(r) = \frac{\delta E_{xc}}{\delta n(r)} \tag{3.18}$$

Given a particular approximation for $E_{xc}(n)$, one obtains $v_{xc}(r)$ and can thus find $v_{eff}(r)$ from $n(r)$ for a given $v(r)$ The set of equations described above is called the KohnSham equations of DFT [63].

The Kohn-Sham equations achieve reasonable correspondence with experiment when applied

to single atoms. The best LDA calculations provide more accurate results than the Hartree-Fock approximation and approach the accuracy demanded by quantum chemists; surveys comparing computations in molecules with experimental results. Many different types of approximations have been tried to bring density functional theory into as close correspondence with experiment as possible. For example, the generalized gradient approximations (GGA) add extra derivative terms. The pure research problem of painstakingly finding accurate solutions to the electronic energy of jellium thus turned out to have much more practical importance than one might have expected from such a simplified model system. From the quantum Monte Carlo calculations in jellium, it was possible to find the energy of the electron gas as a function of density.

3.4.1 Solving the Kohn-Sham equations

Once we have approximated the exchange-correlation energy, we are in a position to solve the Kohn-Sham equations. The Kohn-Sham equations have an iterative solution; they have to be solved self-consistently. To solve the Kohn-Sham equations for a many body system, we need to define the Hartree potential and the exchange-correlation potential, and to define the Hartree potential and the exchange-correlation potential, we need to know the electron density $n(r)$. By using independent-particle methods, the KS equations provide a way to obtain the exact density and energy of the ground state of a condensed matter system. The KS Given that the effective KS potential V_{KS} and the constant KS, equations must be consistently solved. n(r) and electron density are closely linked terms. This is usually done numerically through some self-consistent iterations as shown in Figure 3.1. The process starts with an initial electron density, usually a superposition of atomic electron density, then the effective KS potential V_{KS} is calculated and the KS equation is solved with single-particle eigenvalues and wavefunctions, a new electron density is then calculated from the wavefunctions. After this, self-consistent condition(s) is checked. Self-consistent condition(s) can be the change of total energy or electron density from the previous iteration or total force acting on atoms is less than some chosen small quantity, or a combination of these individual conditions. If the self-consistency is not achieved, the calculated electron density will be mixed with electron density from previous iterations to get a new electron density. A new iteration will start with the new electron density. This process continues until self-consistency is reached. After the self-consistency is reached, various quantities can

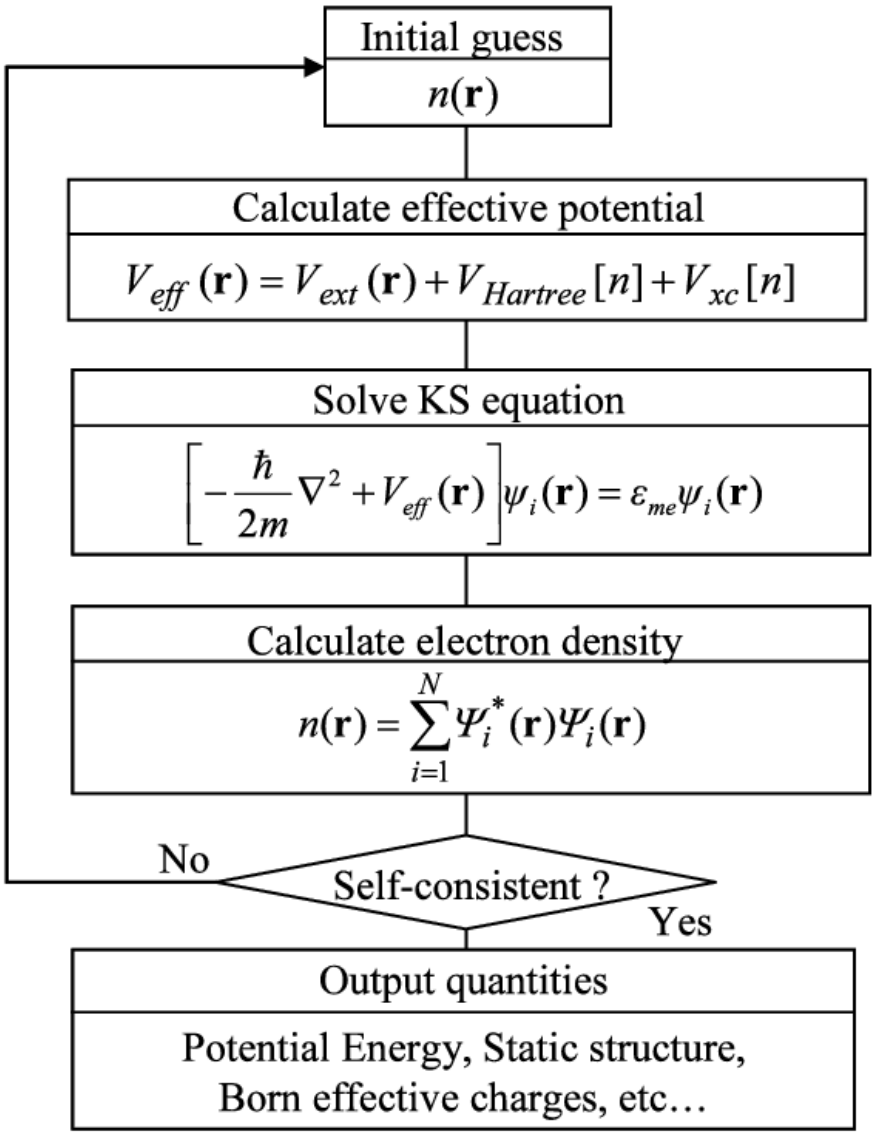

Figure 3.1: Illustration of the self-consistent field (SCF) procedure for solving the Kohn-sham equations.

be calculated including total energy, forces, stress, eigenvalues, electron density of states, band structure, etc..

Solving the Kohn-Sham equation with a given Kohn-Sham potential V_{KS} is the phase that takes up the most time in the entire procedure. When boundary conditions are used, there are numerous different methods for calculating the independent particle electronic states in solids. They are basically classified into three types :

1.Plane waves.

In this method, the wave functions (eigenfunctions of the KS equations) are expanded in a complete set of plane waves and the external potential of nuclei are replaced by pseudopotentials which include effects from core electrons. Such pseudopotentials have to satisfy

certain conditions. Most widely used pseudopotentials nowadays include norm conserving pseudopotentials (NCPPs) and ultrasoft pseudopotentials (USPPs). In norm-conserving pseudopotentials, five requirements should be satisfied:

The pseudo valence eigenvalues should agree with all-electron valence eigenvalues for the chosen atomic reference configuration. The pseudo valence wavefunctions should match all-electron valence wavefunctions beyond a chosen core radius R_c. The logarithmic derivatives of the pseudo and the all-electron wavefunctions should agree at R_c . The integrated charge inside R_c for each wavefunction agrees (norm-conservation) and the first energy derivative of the logarithmic derivatives of the all-electron and pseudo wavefunctions agree at R_c , and therefore for all $r \leq R_c$.

In ultrasoft pseudopotentials, the norm-conservation condition is not required so that the pseudo wavefunctions are much softer than pseudo wavefunctions in norm conserving pseudopotentials. As a result, it significantly reduces the number of plane waves needed to expand the wavefunctions (smaller energy cutoff for wavefunctions).

Plane waves have played an important role in the early orthogonalized plane wave (OPW) calculations and are generalized to modern projector augmented wave (PAW) method. Because of the simplicity of plane waves and pseudopotentials, computational load is significantly reduced in these methods and therefore it is most suitable for calculations of large systems. In this method, forces can be easily calculated and it can be easily developed to quantum molecular dynam- ics simulations as well as response to (small) external perturbations. However, results from plane wave methods using pseudopotentials are usually less accurate than results from all-electron full potential methods. And great care should be taken when one generates a pseudopotential and it should be tested to match results from all-electron calculations. The most widely used codes using plane waves and pseudopotentials are plane wave self-consistent field (now known as Quantum ESPRESSO) (PWscf), ABINIT , VASP (which uses PAW method too).

2. Localized atomic(-like) orbitals.

The most well-known methods in this category are linear combination of atomic orbitals (LCAO), also called tight-binding (TB) and full potential non-orthogonal local orbital (FPLO). The basic idea of these methods is to use atomic orbitals as the basis set to expand the one-electron wavefunction in KS equations.

In FPLO, in addition to the spherical average of the crystal potential, a so-called confining

potential $V_{con} = (r/r_0)^m$ is used to compress the long range tail of the local orbitals (wave functions), where m is the confining potential exponent with a typical value of four, $r_0 = (x_0 rNN/2)^{3/2}$ is a compression parameter with x_0 being a dimensionless parameter and rNN the nearest neighbor distance. Therefore, the atomic-like potential is written as

$$V_{at}(r) = -(\frac{1}{4\pi}) \int V(r - R - \tau) d^3r + V_{con}(r) \tag{3.19}$$

where the first term is the spherical average of the crystal potential mentioned above. For systems containing atom(s) with partially filled 4f and 5f shells, the confining potential exponent m needs to be increased to 5 or 6. In practice, the dimensionless parameter x_0 is taken as a variational parameter in the self-consistent procedure.

3. Atomic sphere methods.

Methods in the class can be considered as a combination of plane wave method and localized atomic orbitals. It uses localized atomic orbital presentation near the nuclei and plane waves in the interstitial region. The most widely used methods are (full potential) linear muffin-tin orbital (LMTO) as implemented in LMTART by Dr. Savrasov and (full potential) linear augment plane wave (LAPW) as implemented in WIEN2k.

However, to find the electron density, we must know the single electron wave functions. We do not know these wave functions until we solve the Kohn-Sham equations. The well-known approach to solve the Kohn-Sham equations is to start with an initial trial electron density as illustrated in Figure 3.1. Then solve these equations using the trial electron density. After solving the Kohn-Sham equations, we will have a set of single electron wave functions. Using these wave functions, we can calculate the new electron density. The new electron density is an input for the next cycle. Finally, compare the difference between the calculated electron densities for consec- utive iterations. If the difference in electron density between consecutive iterations is lower than an appropriately chosen convergence criterion, then the solution of the Kohn-Sham equations is said to be self-consistent. Now the calculated electron density is considered as the ground state electron density, and it can be used to calculate the total energy of the system [64].

3.5 The Exchange-Correlation Functionals

The major problem in solving the Kohn-Sham equations is that the true form of the exchange-correlation functional is not known. Two main approximation methods have been implemented to approximate the exchange correlation functional. The local density approximation (LDA) is the first approach to approximate the exchange-correlation functional in DFT calculations. The second well known class of approximations to the Kohn-Sham exchange correlation functional is the generalized gradient approximation (GGA). In the GGA approximation the exchange and correlation energies include the local electron density and the local gradient in the electron density [64].

3.5.1 Local Density Approximation (LDA)

The simplest approximation to the exchange-correlation functional is the local density approximation (LDA) [65]. The local density approximation is based on the assumption that at every point in the molecule the energy density has the value that would be given by a homogeneous electron gas which had the same electron density r at that point. The energy density is the energy (exchange plus correlation) per electron. Note that the LDA does not assume that the electron density in a molecule is homogeneous (uniform); that drastic situation would be true of a Thomas-Fermi molecule, which, as we said above, cannot exist. The term local was used to contrast the method with ones in which the functional depends not just on r but also on the gradient (first derivative) of r, the contrast apparently arising from the assumption that a derivative is a nonlocal property. However, under the mathematical definition above a gradient is local, and in fact DFT methods formerly called nonlocal are now commonly designated as gradient -corrected. LDA functionals have been largely replaced by a family representing an extension of the method, local spin density approximation (LSDA; below) functionals. In fact, in extolling the virtues of a systematic nonempirical ascent of the DFT Jacobs ladder, Perdew et al. slight LDA and assign to the lowest rung LSDA functionals [66].

As a practical approximate expression for$E_{xc}[n]$, Kohn and Sham suggested what is known in the context of DFT as the local density approximation, or LDA:

$$E_{xc}[n(r)] \simeq \int drn(r)\epsilon_{xc}(n(r))) \tag{3.20}$$

where $\epsilon_{xc}(n)$ is the exchangecorrelation energy per electron in a uniform electron gas of density n. This quantity is known exactly in the limit of high density, and can be computed accurately at densities of interest, using Monte Carlo techniques (i.e. there are no free parameters). In practice one usually employs parametric formulas, which are fitted to the data and are accurate to within ..

Note that the only difference between the resulting computational scheme and a naive mean-field approach is the addition of the potential

$$v_{xc}(r) = \frac{d(n\epsilon_{xc}(n))}{dn}|_n = n(r) \tag{3.21}$$

to the electrostatic potential at the appropriate step in the selfconsistency loop. The corresponding expression for the groundstate energy is:

$$E_0 = \sum_{i=1}^{N} \epsilon_i - E_{es}[n(r)] + \int drn(r)(\epsilon_{xc}(n(r)) - v_{xc}(n(r)) \tag{3.22}$$

The first term is the noninteracting energy, the second term is half of the Hartree scheme's double counting of the electrostatic energy, and the last term is a similar subtraction for the exchangecorrelation energy. The LDA has been shown to give very good results for many atomic, molec- ular and crystalline interacting electron systems, even though in these systems the density of electrons is not slowly varying [67]. The advantage of the homogeneous electron gas model is that it is the only system where the E_{xc} functional is known accurately. In strictly theoretical sense the local approximation is only justified when the density is slowly changing. However, although the densities in atoms and molecules are typ- ically highly inhomogeneous, LDA still gives surprisingly good results. It has been found, that LDA gives reasonably good results for equilibrium structures, harmonic frequencies and dipole moments in molecules [65].

3.5.2 Generalized-Gradient Approximation (GGA)

As mentioned above, the LDA neglects the inhomogeneities of the real charge density which could be very different from the HEG. The XC energy of inhomogeneous charge density can be significantly different from the HEG result. This leads to the development of various generalized-gradient approximations (GGAs) which include density gradient corrections and higher spatial derivatives of the electron density and give better results than LDA in many

cases. Three most widely used GGAs are the forms proposed by Becke (B88), Perdew et al and Perdew, Burke and Enzerhof (PBE). The definition of the XC energy functional of GGA is the generalized form of LSDA to include corrections from density gradient $n(r)$ as

$$E_{XC}^{GGA}[n\uparrow(r), n\downarrow(r)] = \int n(r)\epsilon_X^{hom}(n(r))F_{XC}(n\uparrow(r), n\downarrow(r), |\bigtriangledown n\uparrow(r)|, |\bigtriangledown n\downarrow(r)|, ...)dr \tag{3.23}$$

where ϵ_{XC} is dimensionless and $\epsilon_X^{hom}(n(r))$ is the exchange energy density of the unpolarized HEG.F_{XC} can be decomposed linearly into exchange contribution F_X and correlation contribution F_C as $F_{XC} = F_X + F_C$.For a detailed treatment of F_X and F_C in different GGAs. In general, GGA outperforms LDA in predicting bond length and binding energy of molecules, crystal lattice constants, and other properties, especially in systems with rapidly fluctuating charge density. GGA, on the other hand, has a tendency to overcorrect. The lattice constants from LDA calculations correspond well with experimental data in ionic crystals, however GGA will overestimate it. Nonetheless, in materials where electrons are confined and strongly correlated, such as transition metal oxides and rare-earth elements and compounds, both LDA and GGA function poorly. This flaw causes approximations that go beyond LDA and GGA .

3.5.3 PBE-GGA (Perdew-Burke-Ernzerhof) Approximation

The PBE form is probably the simplest GGA functional. Hence we give it as an explicit example. The reader is referred to other sources such as the paper on Comparison shopping for a gradient-corrected density functional, by Perdew and Burke. The PBE functional for exchange is given by a simple form for the enhancement factor F_x.The form is chosen with $F_x(0) = 1$ (so that the local approximation is recovered) and F_x constant at large s,

$$F_x(s) = 1 + \kappa - \kappa/(1 + \mu s^2/\kappa) \tag{3.24}$$

where $\kappa = 0.804$ is chosen to satisfy the LiebOxford bound. The value of $\mu = 0.21951$ is chosen to recover the linear response form of the local ap- proximation, i.e. it is chosen to cancel the term from the correlation. This may seem strange, but it is done to agree better with quantum Monte Carlo calculations. This choice violates the known expansion at low s given in Eq. (3.23), with the rationale of better fitting the entire functional. Correlation takes the form of a local correlation and an additive term, both of which are dependent on

gradients and spin polarization.

The form chosen to satisfy a number of requirements is

$$E_c^{GGA-PBE}[n\uparrow, n\downarrow] = \int d^3rn[\epsilon_C^{hom}(r_s,\zeta) + H(r_s,\zeta,t)] \tag{3.25}$$

where $\zeta = (n\uparrow, n\downarrow)/n$ is the spin polarization,r s is the local value of the density parameter, and t is a dimensionless gradient $t = |\nabla n|/(2\phi\kappa_{TF}n)$.Here $\phi = ((1+\zeta)^{\frac{2}{3}} + (1-\zeta)^{\frac{2}{3}})/2$ and t is scaled by the screening wavevector k_{TF} rather than k_F . The final form is

$$H = \frac{e^2}{a_0}\gamma\phi^3 log(1 + \frac{\beta}{\gamma}t^2\frac{1+At^2}{1+At^2+A^2t^4}) \tag{3.26}$$

where the factor e^2/a_0, with a_0 the Bohr radius, is unity in atomic units. The function A is given by [32]

$$A = \frac{\beta}{\gamma}[exp(\frac{(-\epsilon_c^{hom}}{\gamma\phi^3\frac{e^2}{a_0}}) - 1]^{-1} \tag{3.27}$$

Chapter 4

Results and Discussion

In this work, Ni and Cd based compounds were studied by means of ab initio methods. DFT calculations were performed based on the full-potential linearized augmented plane wave (FP-LAPW) method as implemented in WIEN2k code [68]. The Perdew-Burke-Ernzehof (PBE) functional [69, 70] with the Generalized Gradient Approximation (GGA) were used for the exchange and correlation interaction. The wavefunctions of the muffin-tin model's interstitial regions were modified using Fourier series, whilst the wavefunctions of the model's muffin-tin spheres were approximated using spherical harmonic functions. We use the generalized gradient approximation (GGA) to optimize the parameters namely, RKmax, K-Point and lattice constant [71]. After optimization of structure, we set RKmax = 8.5 , 8.0, 7.5 and 8.0 for the compounds Ni_2NbSi , Ni_2ZrGe, Cd_2MnAs and Cd_2MnSb respectively, where R is the smallest muffin tin radii in the unit cell and Kmax is the biggest reciprocal lattice vector employed in the flat wave-function expansion. The convergence of the total energy to a minimum value of 10^{-4} Ry determines the convergence of self-consistency calculations, while the charge convergence criteria was set 10^{-3} e. Furthermore, the number of k-points in the Brillouin zone is selected to 50000.

4.1 Structural properties of Ni-based alloys

Full Heusler compounds form two prototype structures. The regular Heusler crystallizes in a cubic structure $AlCu_2Mn$ prototype with the space group (225, $FM\bar{3}m$) and the inverse Heusler, while in $CuHg_2Ti$ with space group (216, $F4\bar{3}m$). In this work, we will study the full Heusler Ni_2NbSi and Ni_2ZrGe consent with $AlCu_2Mn$ type structure, where Ni atoms occupy A (0, 0, 0) and C (0.5, 0.5, 0.5) Wyckoff positions while Nb, Zr and Si, Ge atoms are respectively located at B (0.25, 0.25,

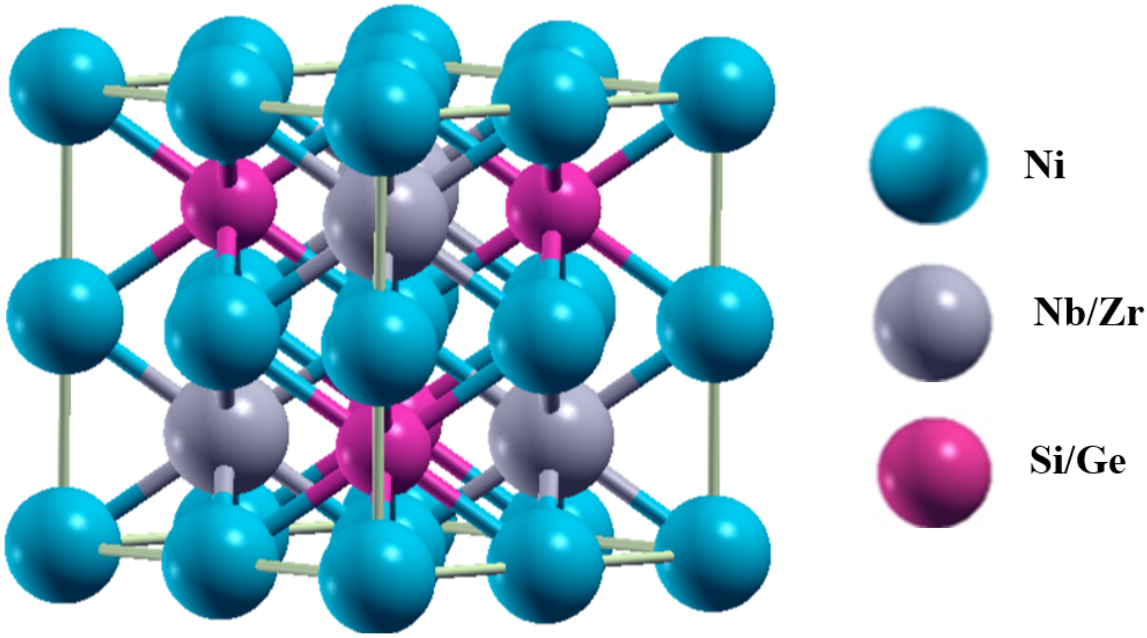

Figure 4.1: Crystal structure of Ni_2NbSi and Ni_2ZrGe full-heusler alloys.

0.25) and D (0.75, 0.75, 0.75) positions. Figure 4.1 gives a representation of this configuration. The crystal structure of both compounds Ni_2NbSi and Ni_2ZrGe are same aspect. The XCrySDen software was used to draw the crystalline structure. In order to obtain ground state of Ni_2NbSi and Ni_2ZrGe alloys, we firstly study the structural property using the plane-wave ultrasoft pseudo-potential DFT method. The volume versus total energy plots of Ni_2NbSi and Ni_2ZrGe alloys are shown in Figure 4.2. The most stable structure of Ni_2NbSi and Ni_2ZrGe is confirmed by optimizing total energy as a function of volume for states with the appropriate lattice parameter. Figure 4.2, depicts the change of total energy with respect to cell volume in ferromagnetic states. Lattice constant is obtained from E-V, energy versus volume diagram where V is equilibrium volume. The parameters we used for calculation are listed in Table 4.1.

Table 4.1: Lattice parameter used in SCF calculation and Fermi energy (eV) of Ni_2NbSi and Ni_2ZrGe compounds using PBA-GGA potential.

Compounds	Optimized lattice parameter (Å)	Fermi energy (eV)
Ni_2NbSi	5.9338	0.8790534861
Ni_2ZrGe	6.1347	0.6672853688

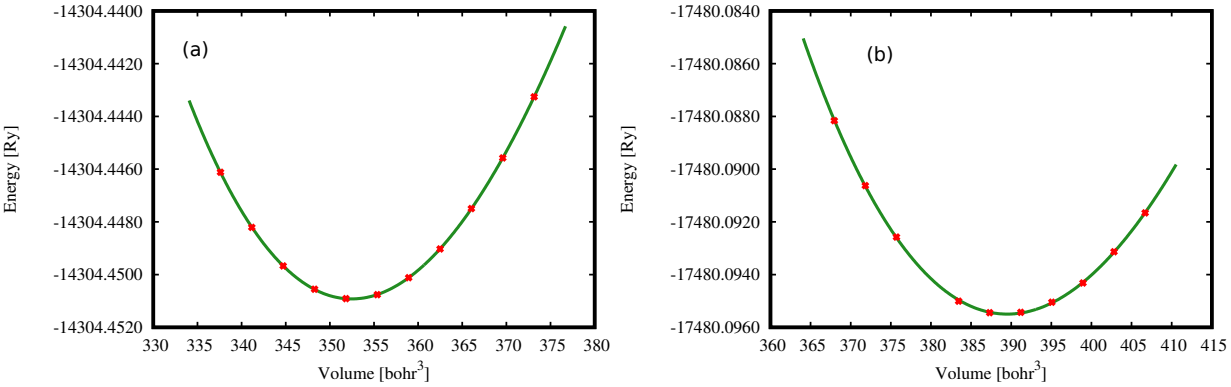

Figure 4.2: Energy versus volume optimization curves for (a) Ni_2NbSi and (b) Ni_2ZrGe .

We also determined band gap, total energy, and Fermi energy through the SCF calculation.

4.2 Band structure of Ni-based alloys

The investigation of the electronic band structure is necessary to understand the physical properties of crystaline solids which almost completely describe optical as well as transport properties. Spin-

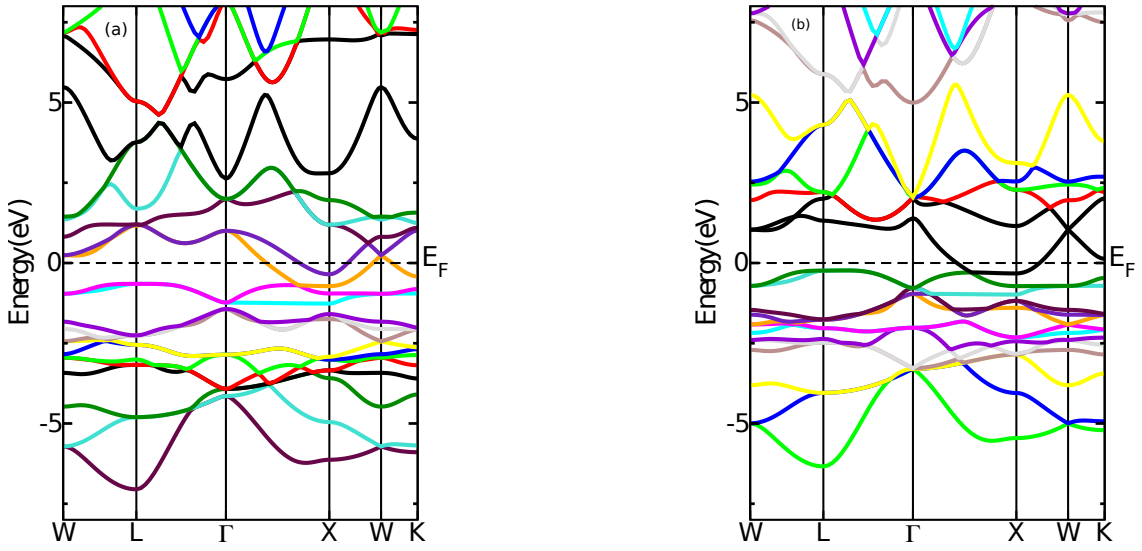

Figure 4.3: Estimated Band Structure of (a) Ni_2NbSi and (b) Ni_2ZrGe

polarized band structure of Ni based two compounds at the 5.9338 Å and 6.1347 Å lattice constant for both the spin-up and spin-down channels at equilibrium state along the high symmetry direction in the first Brillouin zone are illustrated in Figure 4.3(a) the band structure of Ni_2NbSi and the Figure 4.3(b) the band structure of Ni_2ZrGe respectively. Fermi level is set to zero. For the both alloys, it's evidant that the valence bands overlap with conduction bands in both spin-up and spin-down band structure and the Fermi level passes through the overlapping region E_F. So the band gap is zero here.

4.3 Density of States (DOS) of Ni-based alloys

The number of unique states that electrons can occupy at a given energy level, or the number of electron states per unit volume per unit energy, is known as the density of states (DOS). The bulk properties of conductive substances, such as specific heat, paramagnetic susceptibility, and other transport phenomena, are controlled by this function.

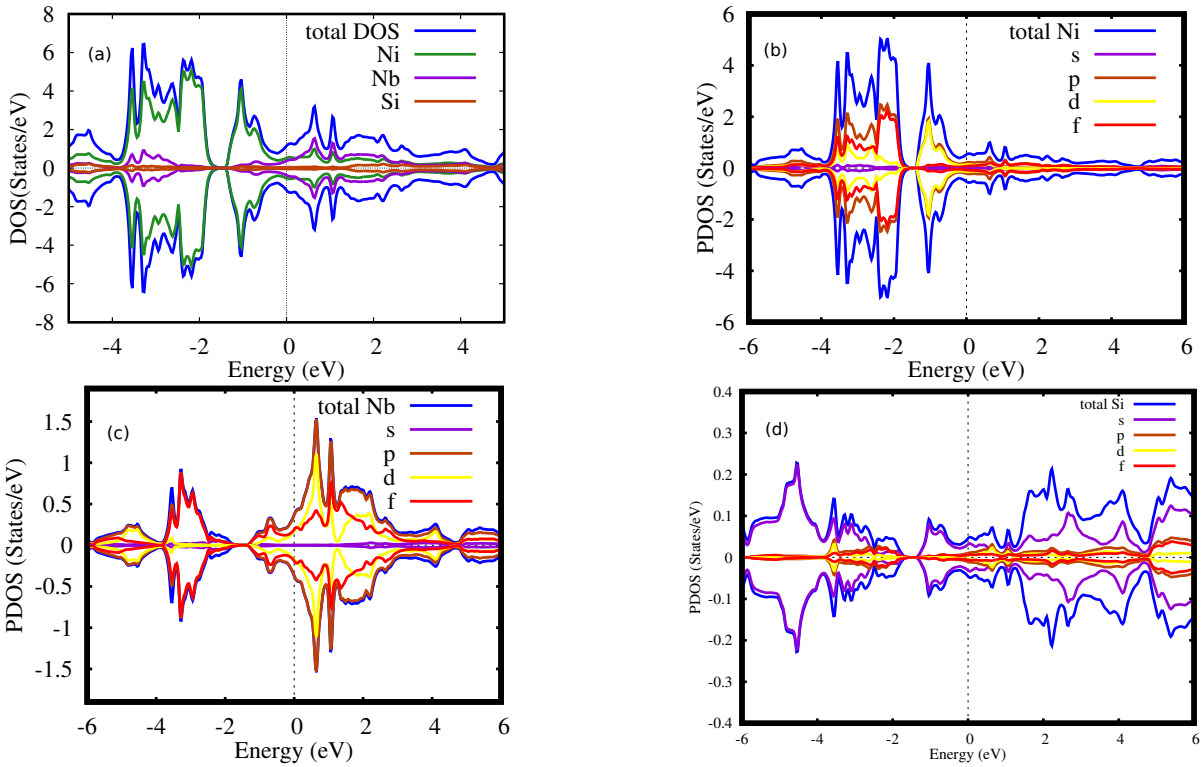

Figure 4.4: (a) total density of states (TDOS) and partial density of states (PDOS) of Ni_2NbSi (b) Ni (c) Nb and (d) Si atoms

For detailed investigations of the formation of energy bands, one needs to compute the density of states (DOS) of the system. The total and partial DOS must be computed with GGA in order to examine the electronic characteristics of materials. The total and partial densities of states for Ni_2NbSi and Ni_2ZrGe are depicted in Figure 4.4 and Figure 4.5. Now, the PDOS of Ni contains the orbital of electrons for the spin up and spin down for Ni_2NbSi and Ni_2ZrGe alloys are plotted in Figure 4.4(b) and Figure 4.5(b). Similarly the PDOS of Nb and Si are also plotted in Figure 4.4(c) and Figure 4.4(d). And the PDOS of Zr and Ge are also plotted in Figure 4.5(c) and Figure 4.5(d). The upper portion displays the majority spin density, while the lower portion displays the minority spin density. For Ni_2NbSi alloys, in Figure 4.4(c) the conduction band overleps the Fermi level and enters into the valance band region. Similarly For Ni_2ZrGe alloys also the conduction band overleps the Fermi level and enters into the valance band region. So this case indicates that the both systems are full metallic.

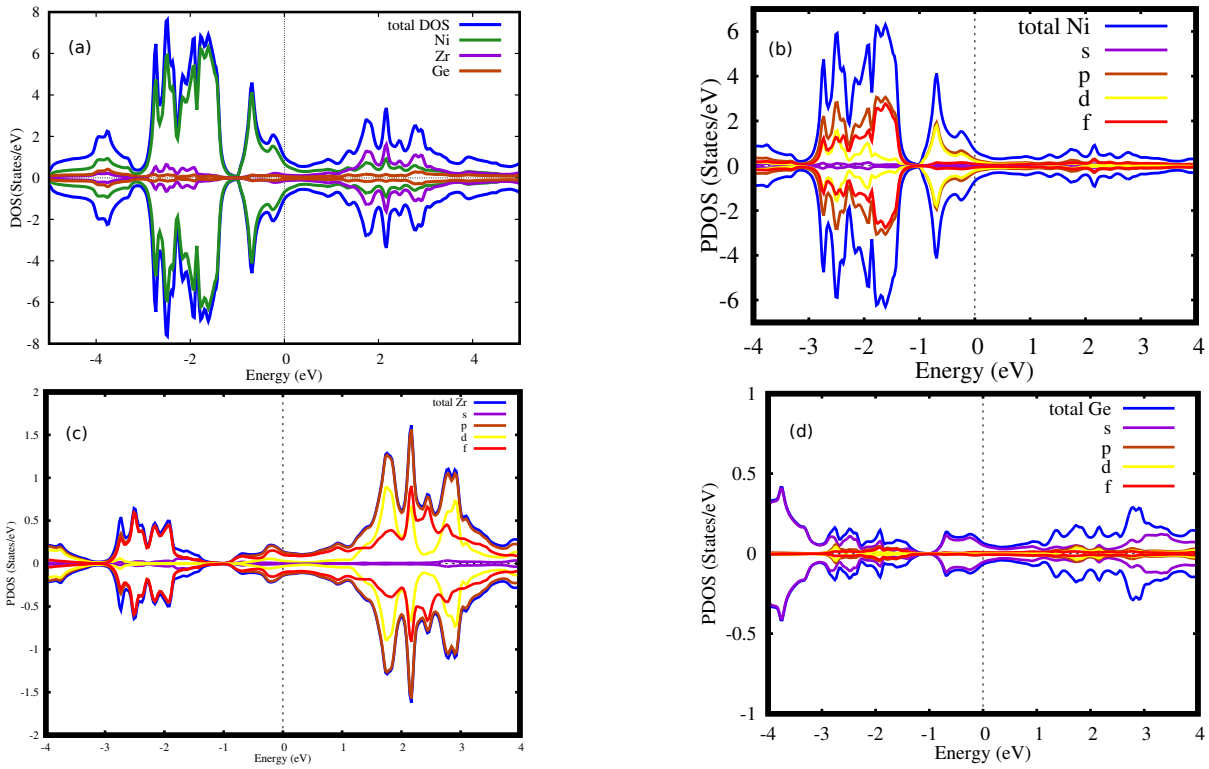

Figure 4.5: (a) total density of states (TDOS) and partial density of states (PDOS) of Ni_2ZrGe (b) Ni (c) Zr and (d) Ge atoms

4.4 Optical Properties of Ni-based alloys

The term optical property describes a material's behavior when electromagnetic radiation (light) is incident on the material's surface or, in other words, how a material interacts under an incident electromagnetic radiation. The optical properties of matter are studied in optical physics, a subfield of optics. Different types of material show different optical properties due to differences in physical, chemical, and mechanical characteristics. The knowledge of optical properties is very important in various industrial as well as in scientific applications. In the selection of material for the purpose of contactless temperature measurement devices, heat transfer methods, laser technology, etc., complete knowledge of optical properties of materials is necessary for efficient operation. Now, we have calculated the optical parameters of Ni based two compounds. In order to investigate the optical properties of Ni_2NbSi and Ni_2ZrGe full-Heusler compounds, we calculated its absorption coefficient, optical conductivity, optical reflectivity, refractive index, dielectric tensor and electron energy loss.

4.4.1 Dielectric Function

The Dielectric Constant is a measurement of a substance's capacity to store electrical energy in an electric field. The dielectric constant is a complex quantity that may be represented as

$$\epsilon(\omega) = \epsilon_1(\omega) + i\epsilon_2(\omega) \tag{4.1}$$

where, ϵ_1 and ϵ_2 are the real and imaginary parts of the dielectric function. Real dielectric constant respectively, $(\epsilon_1(\omega))$ represents the degree of polarization of a material when it placed into an electric field and imaginary dielectric function $(\epsilon_2(\omega))$ represents the energy dissipation aptitude of a dielectric material. The optical response of the material to an electromagnetic field is described by the dielectric function [73]. The real and imaginary dielectric function for Ni_2NbSi and Ni_2ZrGe obtained from PBE-GGA potential in Figure 4.6(a,b). From Figure 4.6(a) we say

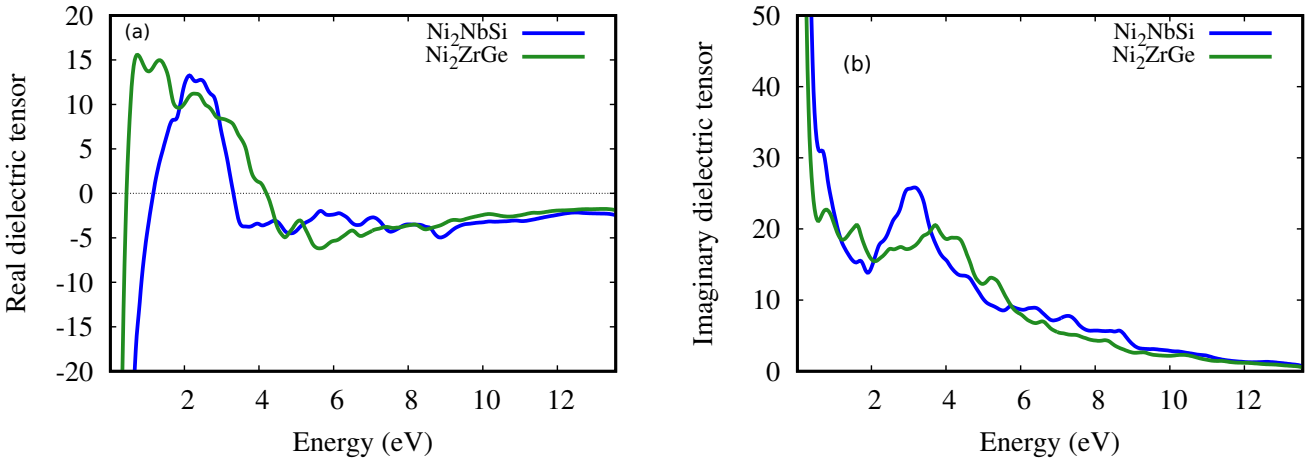

Figure 4.6: Dielectric Funtion for Ni_2NbSi and Ni_2ZrGe (a) real (b) imaginary

that both compounds have no negative real dielectric tensors before 3 eV energy. so we use these compound to store electric energy. After 3 eV energy , the real dielectric tensors starts to decrease and get negative value of real dielectric tensor. For imaginary dielectric tensor in Figure 4.6(b) gives that the imaginary dielectric tensor starts to increase and between 2 eV to 4 eV we can see a sharp peak.

4.4.2 Optical Conductivity

Optical conductivity $\sigma(\omega)$ determines the ability of a medium to initiate a phenomenon of conduction as the electromagnetic radiations try to propagate through it. From Figure 4.7(a) it is clear that, optical conductivity increases as energy increases. The energy between 0.63 eV to 1.5 eV the conductivity starts to decrease. After the visible range region conductivity increases. At zero energy position, we get the highest optical conductivity. Between 2.0 eV to 4.5 eV energy, we get

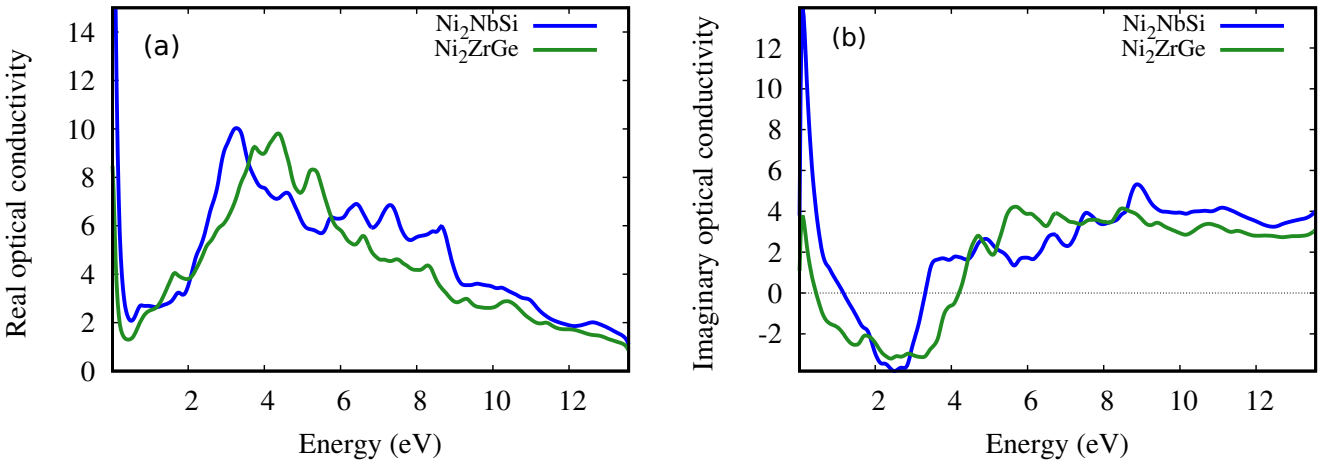

Figure 4.7: Optical conductivity for Ni_2NbSi and Ni_2ZrGe (a) real (b) imaginary

the highest optical conductivity for both compounds. So we say that from Figure both compounds are give the almost same behaviour. For imaginery optical conductuvity from Fig 4.7(b) we can say that, the energy between 2.1 eV to 3 eV the conductivity starts to decrease and becomes almost zero for the Ni_2NbSi compound at point 2.5 eV. But after visible range region conductivity increases. For zero energy position we get the highest optical conductivity for the Ni_2ZrGe compound. The conductivity is high at point 9 eV energy. From these Figure, we can say that Ni_2NbSi compound is better conductor than Ni_2ZrGe compound.

4.4.3 The Absorption Coefficient

The absorption coefficient is used to calculate how far into a material light of a specific wavelength can penetrate before being absorbed. A substance can appear transparent if it is thin enough to barely slightly absorb light of that wavelength. If a substance is thin enough to just very faintly absorb light of a certain wavelength, it can look transparent. When energy levels rise, metal's absorption coefficient rises as well. Generally, metal conductors have a high absorption coefficient. Because light with energy below the band gap does not have enough energy to drive an electron from the valence band into the conduction band, semiconductor materials show a sharp edge in their absorption coefficient. As a result, there is no absorption of this light. The absorption coefficient is not constant for photons with energies above the band gap, although it is still substantially dependent on wavelength. The likelihood of absorbing a photon is proportional to the probability of a photon and an electron interacting in such a way that they migrate from one energy band to the next. As the photon's energy rises, interactions with it aren't limited to electrons with energies around the band gap. As a result, more electrons may interact with the photon, causing it to be absorbed [72]. In Figure 4.8 we see that the absorption coefficent of Ni_2NbSi and Ni_2ZrGe heusler compound. The range of photon energies for visible light is 1.63 eV to 3.26 eV. For both Ni_2NbSi

and Ni_2ZrGe compounds the absorption coefficient is very weak in the visible light region. So we can say that these alloys cannot absorb visible light. But after the visible light region, the absorptivity starts to increase. so both compounds absorbs mainly UV light. As the energy increases the

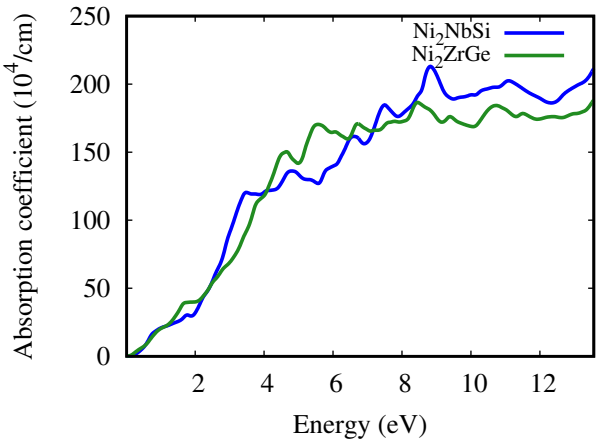

Figure 4.8: Optical absorption coefficient for Ni_2NbSi and Ni_2ZrGe

absorptivity also increases in the region. From the Figure 4.8, we can see that Ni_2NbSi gives a higher absorption coefficent than Ni_2ZrGe. so we can say that, Ni_2NbSi absorbs more light. For melatic compound the absorptivity increases with the energy. Optical absorption provides essential information on the electronic properties of metalic compounds.

4.4.4 Refractive Index

The ratio of the speed of light in a vacuum to the speed of light in the second medium of larger density is used to compute the refractive index (also known as the Index of Refraction). The letter

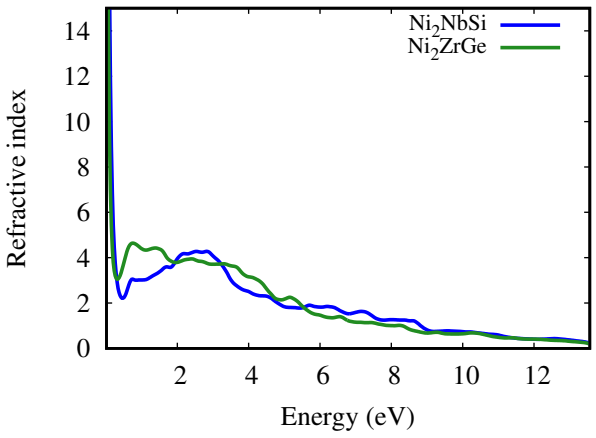

Figure 4.9: Refractive index for Ni_2NbSi and Ni_2ZrGe

'n' is the most popular symbol for the refractive index variable. The greater the deflection (or refraction) of a light beam entering or exiting a material, the higher its refractive index. We are

aware that a material's refractive index indicates how quickly light passes through it. The frequency of light traveling through a medium influences its refractive index (to some extent), with the highest frequencies having the greatest values of n. The correlation between the refractive index and photon energy is shown in Figure 4.9. From these Figure we can see that both compounds Ni_2NbSi and Ni_2ZrGe gives the almost same results. The refractivity is maximum at 0 eV energy and minimum between 10 to 12 eV energy. After 12 eV the refractivity index continuously decrease.

4.4.5 Optical Reflectivity

The reflactance of a material is measured when light is incident on the surface of the material. This is a measurement of a surface's ability to reflect radiation, or the reflectance of a material layer that is thick enough to have a constant reflectance regardless of thickness. Each substance's potential as a perfect absorber is determined by the reflectance and reflectivity spectra. The reflectivity of light from a surface depends upon the angle of incidence and the plane of polarization of the light. The normal incidence reflectivity is dependent upon the indices of refraction of the two media. Analysing the Figure 4.10, we see that at zero energy position the reflectivity is highest but after

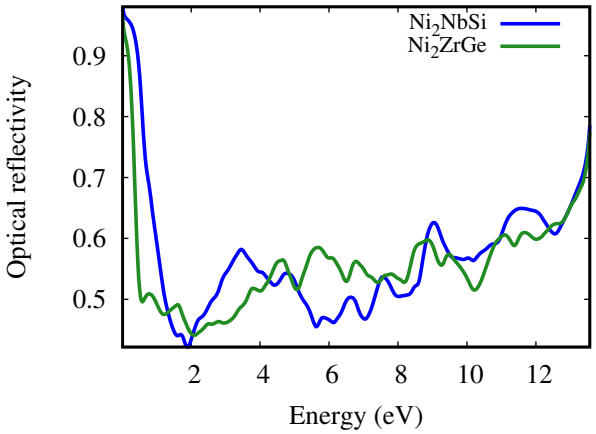

Figure 4.10: Optical Reflectivity for Ni_2NbSi and Ni_2ZrGe

zero position reflectivity starts to decrease and becomes zero at 2 eV position for the Ni_2NbSi. After 2 eV position the reflectivity again starts to increase for both compounds. As the energy increase the reflectivity increase after 2 eV energy. So from this property, we can say that Ni_2NbSi and Ni_2ZrGe are the good metallic reflector in Figure 4.10 is representing the optical reflectivity of Ni_2NbSi and Ni_2ZrGe compounds.

4.4.6 Electron Energy Loss

Energy loss function is the energy lost by a fast-moving electron as it travel through a substance. It's a very significant phase since it offers information about the sample or material's structure and

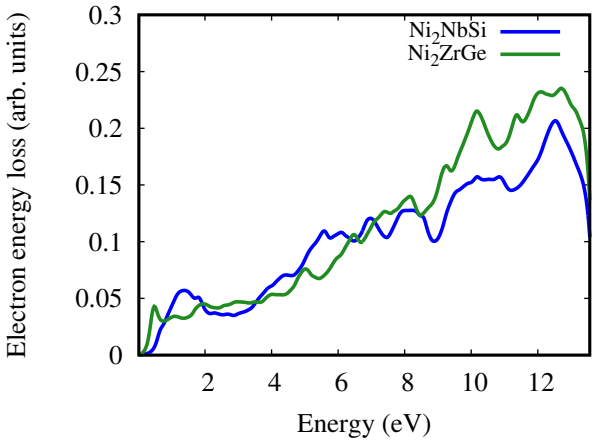

Figure 4.11: Electron energy loss for Ni_2NbSi and Ni_2ZrGe

chemical composition. The electronic energy loss function of a material can be extended from the dielectric function to further characterize the energy loss when electrons flow through a uniform dielectric. From Figure 4.11, we can see that the graph is almost the same for both materials. After 12 eV energy , we have the highest energy loss of about 0.25.

4.5 Structural Properties of Cd-based alloys

we will study the full Heusler Cd_2MnAs and Cd_2MnSb compounds with their structure, where Cd

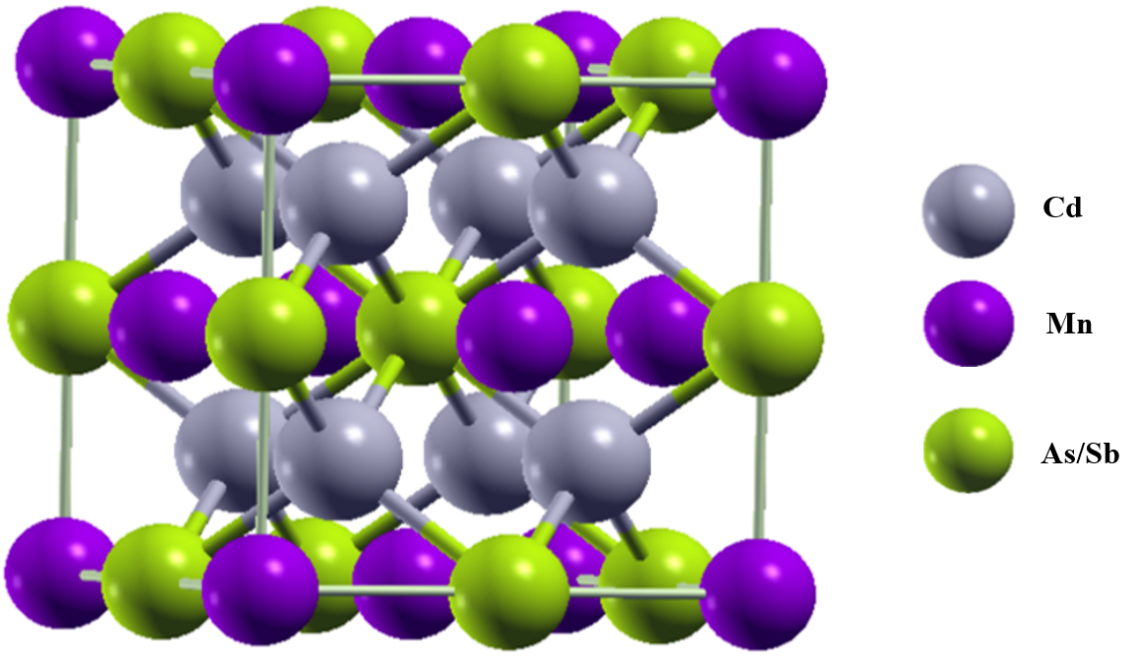

Figure 4.12: Crystal structure of Cd_2MnAs and Cd_2MnSb full-heuslor alloys .

atoms occupy A (0, 0, 0) and C (0.5, 0.5, 0.5) Wyckoff positions while (Mn, As) and (Mn, Sb) atoms are respectively located at B (0.25, 0.25, 0.25) and D (0.75, 0.75, 0.75) positions. Four face-

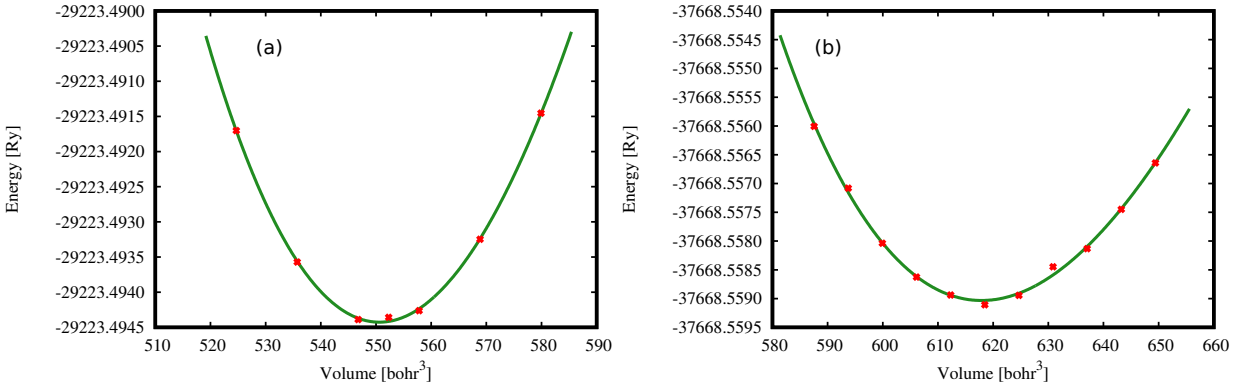

Figure 4.13: Energy versus volume optimization curves of (a) Cd_2MnAs and (b) Cd_2MnSb full-heuslor alloys .

centered-cubic (FCC) lattices are interpenetrating in the full-Heusler compound. Figure 4.12 shows a visual representation of this configuration. By maximizing total energy as a function of volume for states with the lattice parameter are 6.90 Å and 7.15 Å, the most stable structure of Cd_2MnAs and Cd_2MnSb are confirmed. Figure 4.13 depicts the change in total energy in ferromagnetic states with respect to cell volume. The energy against volume (E-V) diagram, where V is the equilibrium volume, is used to determine the lattice constant. Calculated lattice constant and fermi energy are summarized in Table 4.2.

Table 4.2: Lattice parameter used in SCF calculation and Fermi energy of Cd_2MnAs and Cd_2MnSb compounds using PBA-GGA potential.

Compounds	Optimized lattice parameter (Å)	Fermi energy (eV)
Cd_2MnAs	6.90	0.4654020161
Cd_2MnSb	7.15	0.4545148167

4.6 Band Structure of Cd-based alloys

Understanding the physical characteristics of crystalline solids, which nearly entirely define optical as well as transport aspects, requires an analysis of the electronic band structure. The calculation is done by defining highly symmetric points on the edge of the Brillouin zone with sampling path of Γ-X-W-Γ-L-W and W-L-Γ-X-W-K. For both,the compound's energy band lies between -5 eV to 5 eV. The bands that coincide below the Fermi level are referred as the valence band while the band above the reference Fermi line is the conduction band. For these alloys, in order that the valence bands overlap with conduction bands structure, and the Fermi level passes through the overlapping region E_F. In this case, the band gap is zero. The majority spin channel and minority spin channel both have zero flip gaps, proving that these alloys are both truly complete metallic. We may conclude that Cd_2MnAs and Cd_2MnSb are both complete metallic Heusler alloys based

on figure 4.14. These compounds can be used to make electrical lines and other electrical devices since good metal conductors have a zero band gap.

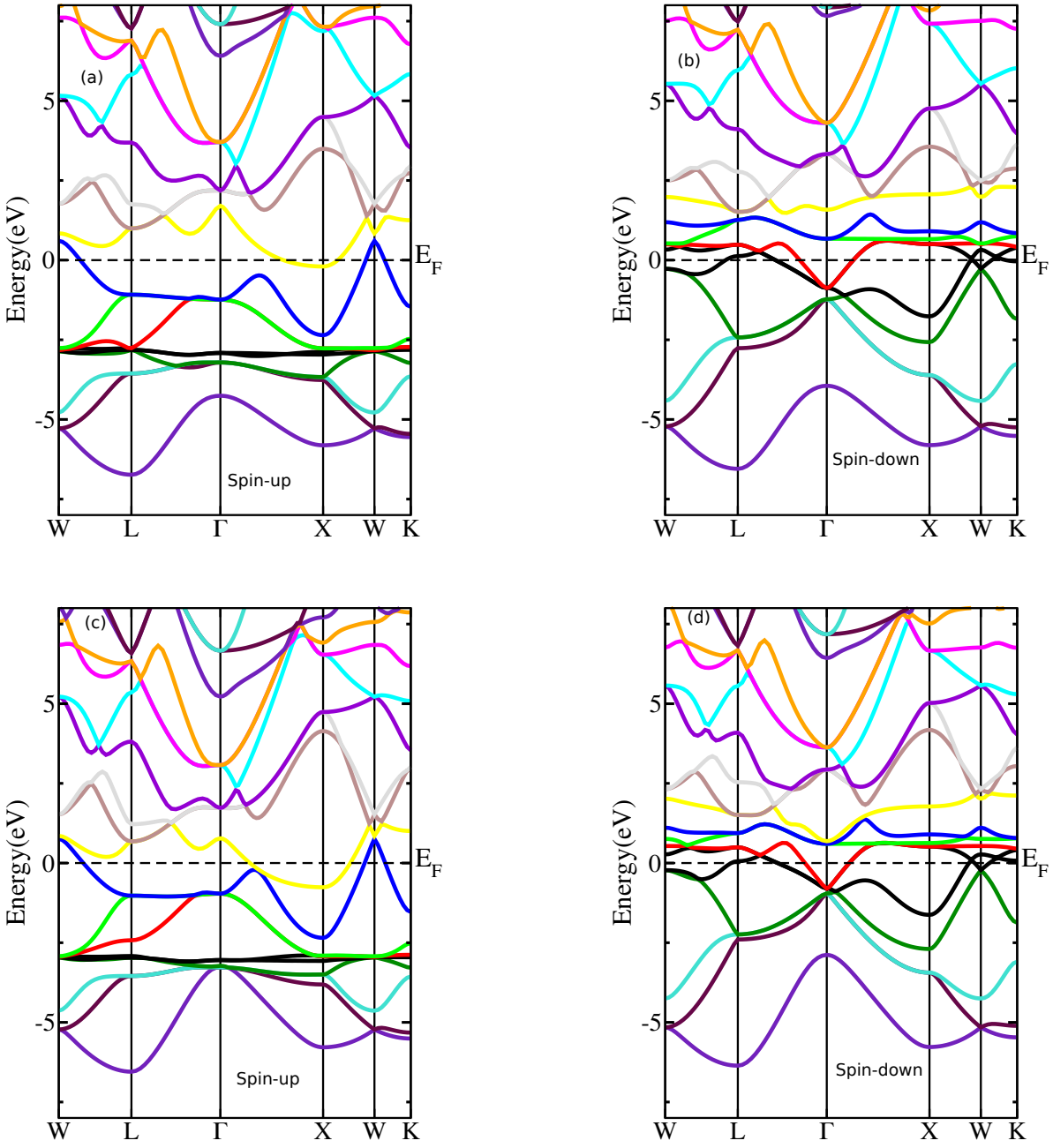

Figure 4.14: Estimated Band Structure of (a,b) Cd_2MnAs and (c,d) Cd_2MnSb

4.7 Density of states (DOS) of Cd-based alloys

The density of states (DOS) is essentially the number of different states that electrons are permitted to occupy at a given energy level, i.e. the number of electron states per unit volume per unit energy.

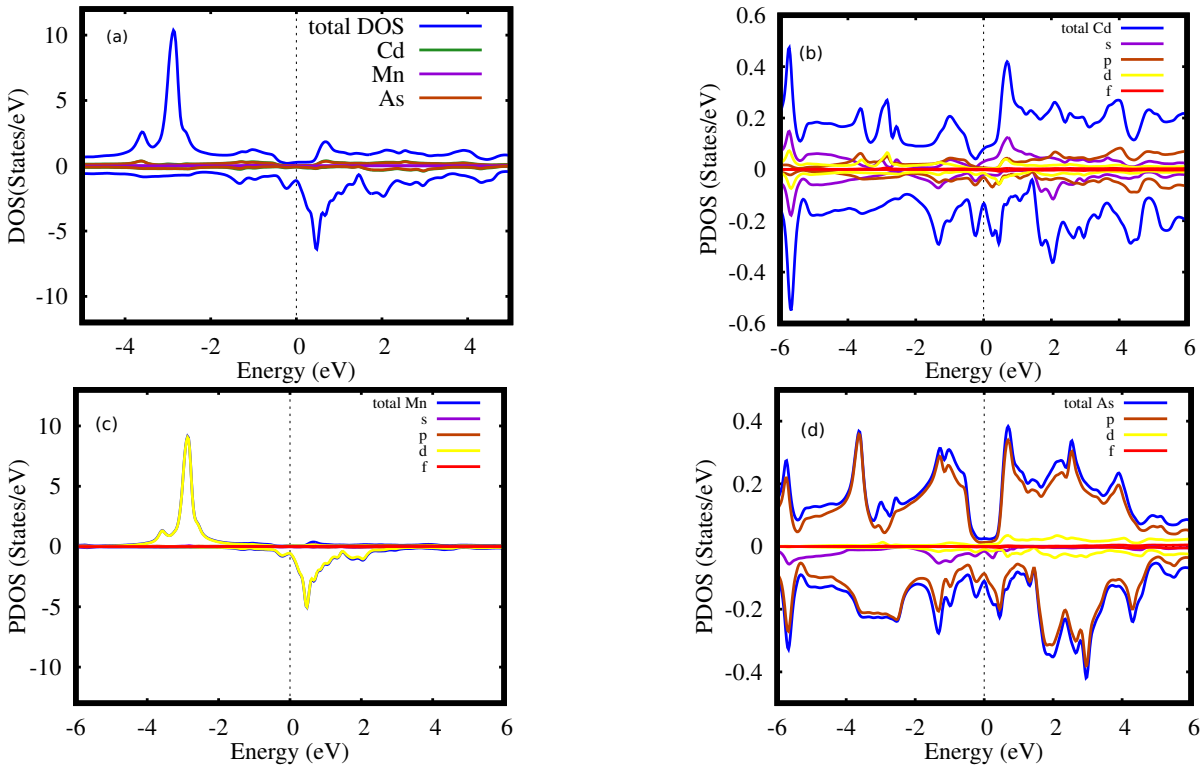

Figure 4.15: (a) total density of states (TDOS) and partial density of states (PDOS) of Cd_2MnAs (b) Cd (c) Mn and (d) AS atoms

For the study of electronic properties of materials, it is necessary to calculated the total density of states (TDOS) and partial density states (PDOS) with GGA. The corresponding total and partial density of states for Cd_2MnAs and Cd_2MnSb are illustrated in Figure 4.15 and Figure 4.16. Now, the PDOS of Cd contains the orbital of electrons for the spin up and spin down for Cd_2MnAs and Cd_2MnSb alloys are plotted in Figure 4.15(b) and Figure 4.16(b). Similarly the PDOS of Mn and As are also plotted in Figure 4.15(c) and Figure 4.15(d). And the PDOS of Zr and Ge are also plotted in Figure 4.16(c) and Figure 4.16(d). The majority spin density is shown in the upper portion, while the minority spin density is shown in the lower portion. For Cd_2MnAs alloys, in Figure 4.15(c) the conduction band overleps the Fermi level and enters into the valance band region. Similarly For Cd_2MnAs alloys also the conduction band overleps the Fermi level and enters into the valance band region. Therefore, this situation suggests that both systems are full Heusler.

4.8 Magnetic Properties of Cd-based alloys

The magnetic ordering of the Cd_2MnAs and Cd_2MnSb is shown by the spin-polarized computations. We estimated the magnetic moment contributions from the interstitial region as well as the partial magnetic moments of the Cd, Mn, and (AS, Sb) atoms, as shown in Table 4.3. The majority of the total magnetic moment is produced by Cd atoms. The partial moments of Mn and (As, Sb) are

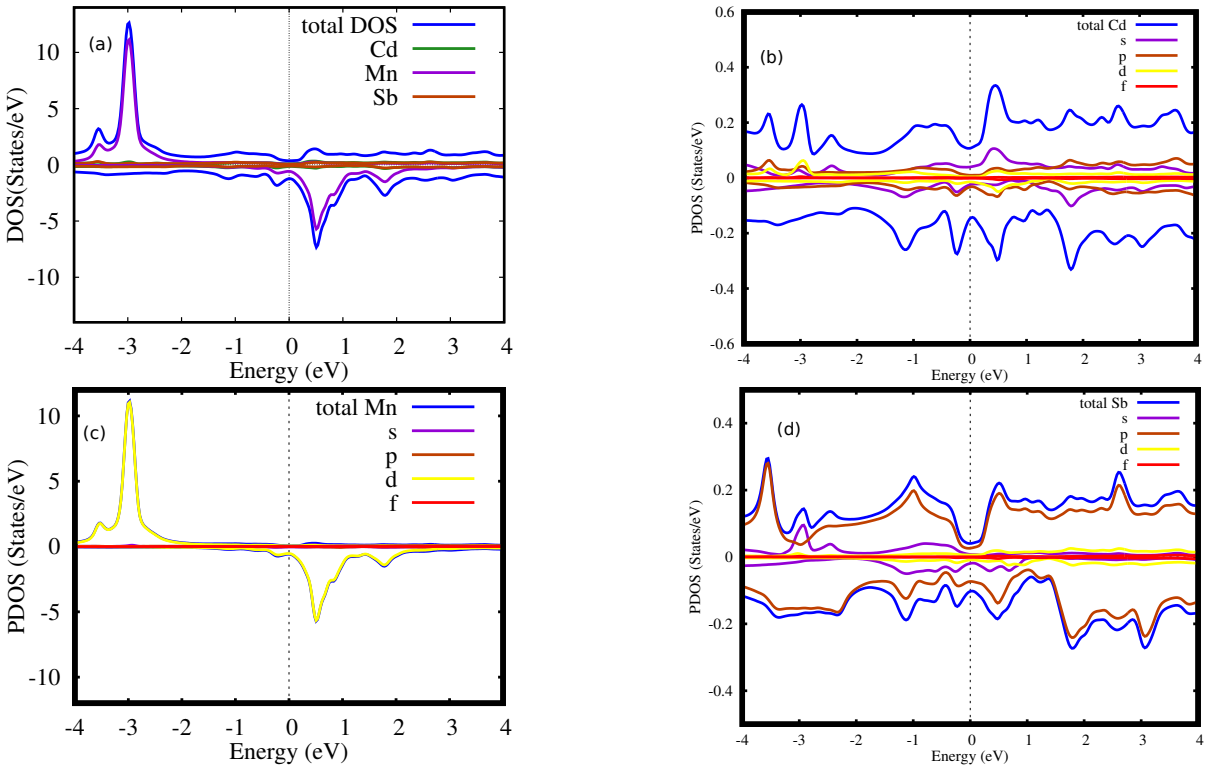

Figure 4.16: (a) total density of states (TDOS) and partial density of states (PDOS) of Cd_2MnSb (b) Cd (c) Mn and (d) AS atoms

Table 4.3: Total spin magnetic moment of Cd_2MnAs and Cd_2MnSb in PBA-GGA approach

Compounds	M_{Cd}/μ_B	M_{Mn}/μ_B	M_{As}/μ_B	M_{int}/μ_B	M_{tot}/μ_B	Magnet type
Cd_2MnAs	-0.05024	3.97162	0.01841	0.10705	3.99661	ferromagnetic
Cd_2MnSb	0.13706	4.11715	0.00789	0.13706	4.19641	ferromagnetic

antiparallel to Cd atoms, proving the ferromagnetic nature of the Cd_2MnAs and Cd_2MnSb alloys. The calculated total magnetic moment for entire Heusler alloys with $L2_1$ structure is an integer quantity in accordance with the Slater-Pauling rule. The Cd atoms benefit from this antiparallel alignment, which results in total magnetic moments of 3.99 μ_B and 4.19 μ_B respectively.

4.9 Optical properties of Cd-based alloys

Solid-state materials exhibit a variety of optical characteristics. In this section, we go through the optical characteristics of Cd_2MnAs and Cd_2MnSb, including their electron energy loss, optical conductivity, optical reflectivity, refractive index, and dielectric tensor. In previous chapter, we have already discussed about the basic concepts of all these optical properties. So in this chapter we will discuss only the basic configuration of these two systems.

4.9.1 Dielectric Function

The dielectric function can be used to describe how an electromagnetic field affects a material's optical response. The real and imaginary dielectric function for Cd_2MnAs and Cd_2MnSb were

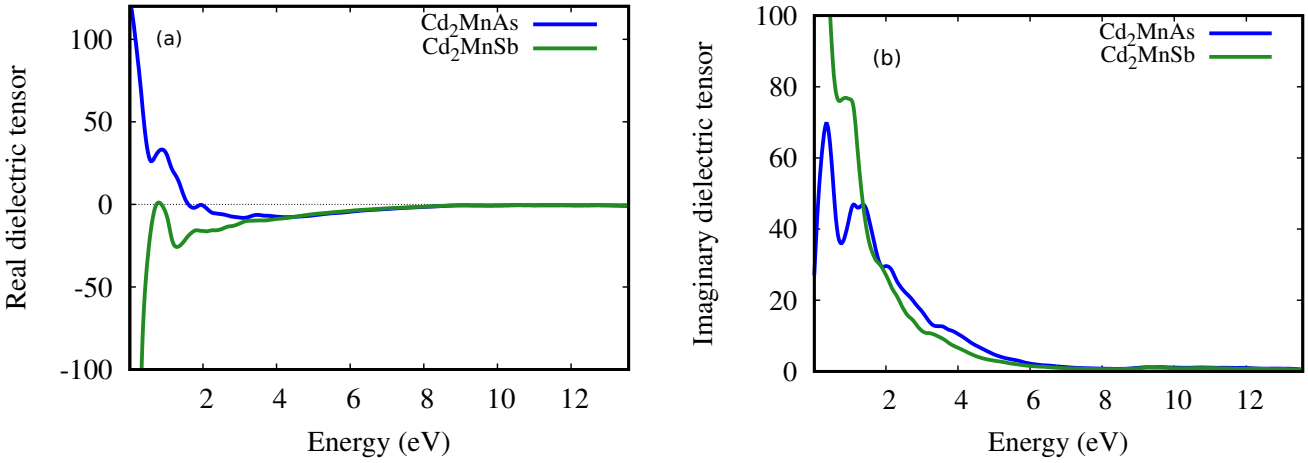

Figure 4.17: Dielectric Funtion for Cd_2MnAs and Cd_2MnSb (a) real (b) imaginary

obtained from PBE-GGA potential in Figure 4.17(a, b) where energy plotted in the X-direction, real and imaginary dielectric function ploted in Y-directin. In Figure 4.17(a) represent the curve for real dielectric function. As can be seen in Figure, the curves in these compounds are opposite configurations in the infrared region. After an energy of 3.8 eV the curves are almost same for both compounds. In Figure 4.17(b) we can see that the imaginary dielectric tensor is high in the infrared region for both compounds. After the visible region the imaginary dielectric tensor decreasees abruptly. In UV region, the value of imaginary dielectric tensor is almost zero.

4.9.2 Optical Conductivity

Optical conductivity is a material property that describes the interaction between the induced current density in the materials and the magnitude of the inducing electric field for arbitrarily selected frequencies. The optical conductivity (real and imaginary) is along with its energy is illustrated in Figure 4.18. From the real optical conductivity curve, it is obvious that the conductivity of Cd_2MnSb is very high and Cd_2MnAs is zero at infrared region. In UV region the conductivity curves are almost same for both alloys. From imaginary conductivity curves, it is clear that the imaginary conductivity is very high at point 0 eV and 3.2 eV for Cd_2MnAs and Cd_2MnSb compounds respectively. After 4 eV energy the imaginary conductivity starts to decrease for both compounds. So we can say that Cd_2MnSb is better conductor than Cd_2MnAs compound.

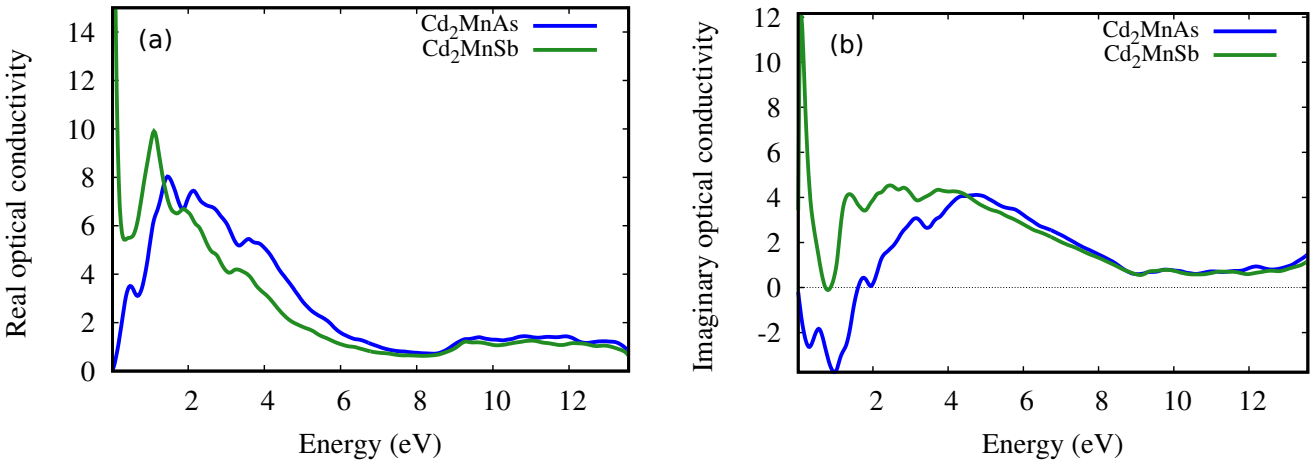

Figure 4.18: Optical Conductivity for Cd_2MnAs and Cd_2MnSb (a) real (b) imaginary

4.9.3 Absorption Coefficient and Electron Energy Loss

In Figure 4.19(a), we can see that the absorption coefficient of Cd_2MnAs and Cd_2MnSb compounds. Absorption coefficient are almost same for both compounds.The value of absorption coefficient

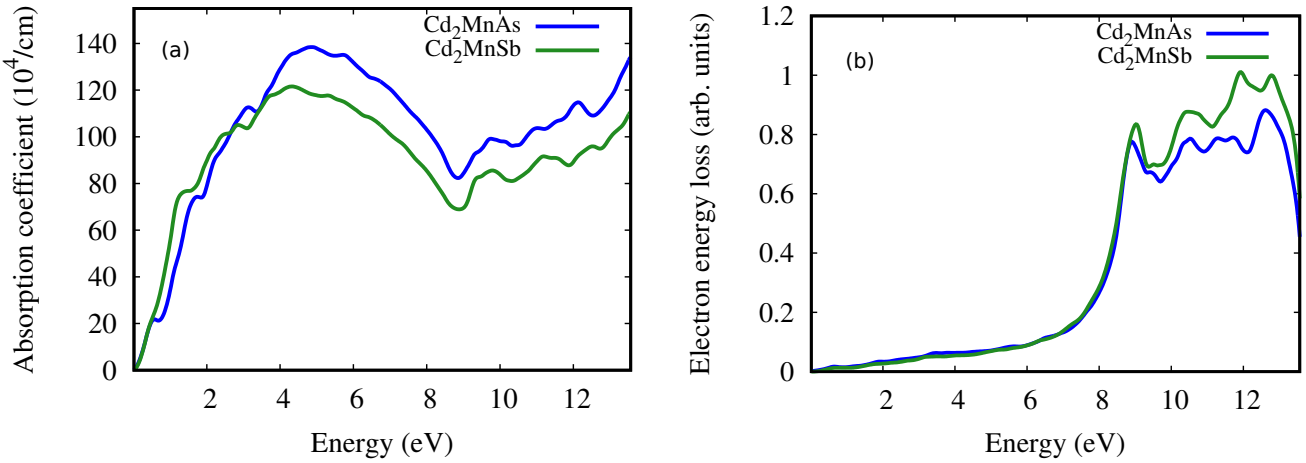

Figure 4.19: Optical Absorption Coefficient (a) and Electron Energy Loss (b) for Cd_2MnAs and Cd_2MnSb

promptily increases when the incident energy becomes higher. In the UV region Cd_2MnAs and Cd_2MnSb have peak valus of 5.1 eV and 4.3 eV respectively. Hence both alloys mainly absorb UV light. So we can say that Cd_2MnAs absorbs more light than Cd_2MnSb compound. Electron energy loss is graphically represent in Figure 4.19(b). Both Cd_2MnAs and Cd_2MnSb compounds have their largest peaks in the UV region. And in infrared region their performance is woefully lacking.

4.9.4 Optical Refractivity and Refractive Index

Material reflectivity is impotant in determining how much light a meterial can reflect in relation to the amount of light. It is exposed to Figure 4.20(a) shows that the reflectivity is higest at 0 eV

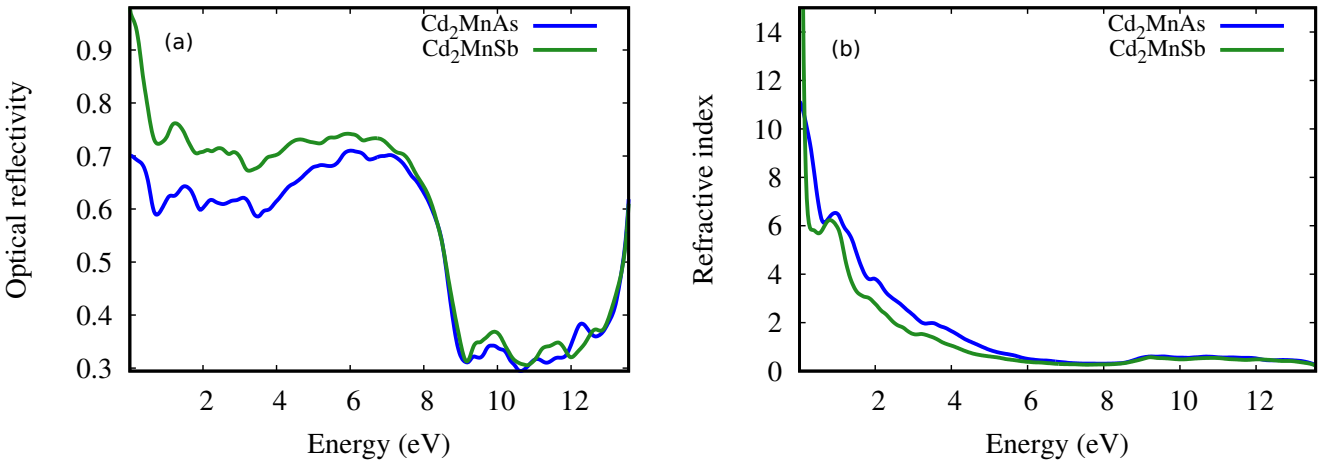

Figure 4.20: Optical Reflectivity (a) and Refractive Index (b) for Cd_2MnAs and Cd_2MnSb

energy position for Cd_2MnSb compound bt after zero position the reflectivity starts to decrease. For Cd_2MnAs compound at first the reflectivity is high but after 7.9 eV energy reflectivity starts to decrease and become zero at 10.8 eV energy. The Optical reflectivity is very high it represents the strong metallic characteristic of the Cd_2MnAs and Cd_2MnSb compounds. In Figure 4.20(b) represent the refractive index vs energy curve. Refractive index is known that the refractive indices are inversely related to the bandgap, if refractive index increases corresponding bandgap decreases. It can be seen that in the lower energy range, there are higher valus of refractive index for both the compounds. This indicates that the metallurgical behavior of both alloys is enhanced.

Chapter 5

Conclusions

In this work, we have studied the structural properties of Ni and Cd based full Heusler alloys using FP-LAPW method as implemented in WIEN2k code with GGA-PBE exchange correlation to investigate their structural, electronic, magnetic, and optical properties. The equillibrium functional constant is found to be 5.93 Å, 6.13 Å, 6.90 Å and 7.15 Å for Ni_2NbSi, Ni_2ZrGe, Cd_2MnAs and Cd_2MnSb respectively. To investigate the electronic properties the diagrams of spin-polarized band structure of Ni and Cd based compounds and DOS, PDOS were plotted. Also found that these compounds for the spin-up and spin-down have no band gap that confirms their metallic properties. The density of states also revealed the metallic nature of these compound. The magnetic moment of Cd based two system are around 4 μ_B , indicating the ferromagnetic contribution of the alloys. In this work, also calculated optical properties, the real and imaginary parts of dielectric function, reflectivity, absorption coefficient and optical conductivity. Curve of the real part of dielectric function versus energy show that there is metallic property in very low energies. At the end, we hope that this effort will be helpful and inspirational to researchers working in this field by emphasizing the merit of further research on all of these substances.

Appendix

The dielectric function describes the responce of a material to the application of an alternating electric field at different photon energy. There are two part of dielectric function; one is real and another is imaginary part. The imaginary part of the dielectric function ignoring all intra-band transitions would be obtained as:

$$Im\varepsilon_{ij}^{[inter]}(\omega) = \frac{h^2e^2}{\pi m_e^2\omega^2}\sum_n \int dk \langle \Psi_k^{c_n}|p^i|\Psi_k^{v_n}\rangle\langle \Psi_k^{v_n}|p^\beta|\Psi_k^{c_n}\rangle\sigma(E_k^{c_n} - E_k^{v_n} - \omega) \tag{5.1}$$

Which includes the summation of inter-band transitions from occupied valence levels with agent-state $|\Psi_k^v\rangle$ and agent-value $E_k^{v_n}$ to unoccupied conduction levels with agent-state $|\Psi_k^{c_n}\rangle$ and agent-value $E_k^{c_n}$ where p stands for momentum operator. The other quantities such as the refraction, absorption, reflection indexes and etc. can be obtained using the real or imaginary parts of the dielectric function. With the help of the imaginary part of dielectric tensor, one can determine the corresponding real part via the Kramers–Kronig relations:

$$Re\varepsilon_{ij}^{[inter]}(\omega) = \sigma_{ij}\frac{2}{\pi}P\int_0^\infty \frac{\bar{\omega}Im\varepsilon_{ij}(\omega)}{\bar{\omega}^2 - \omega^2} \tag{5.2}$$

In which, P indicates the principal value of integral. On the other hand, the contribution of metallic intera-band transitions is obtained as follows

$$Im\varepsilon_{ij}^{[inter]}(\omega) = \frac{\Gamma\omega_{pl,ij}^2}{\omega(\omega^2+\Gamma^2)}, Re\varepsilon_{ij}^{[inter]}(\omega) = \frac{\omega_{pl,ij}^2}{\omega(\omega^2+\Gamma^2)}\omega_{pl}^2 \tag{5.3}$$

In this equation, Γ represents the lifetime broadening in Drude model, ω_{pl} denotes plasma frequency and n indicates electron density. The total dielectric function including all interband and intra-band transitions is obtained as follows:

$$\varepsilon(\omega) = \varepsilon_{ij}^{[inter]}(\omega) + \varepsilon_{ij}^{[intra]}(\omega) \tag{5.4}$$

The energy loss of electron through a fast moving throughout the material is described by Eloss function which related to dielectric function as follows:

$$(Eloss) = L_{ij}(\omega) = -Im\{\frac{1}{\varepsilon_{ij}(\omega)}\} = \frac{Im\varepsilon_{ij}}{(Re\varepsilon_{ij})^2 + (Im\varepsilon_{ij})^2} \tag{5.5}$$

These interactions include intraband and interband transitions, plasmon excitations (free electron oscillations), phonon excitations, inner shell ionization and etc. The energy in which the curve transfers from negative to positive values in the diagram of real part of dielectric function corresponds to the plasmon energy. Another calculated optical parameter is coefficient:

$$R(\omega) = R_{ij}(\omega) = \left[\frac{(Re\varepsilon_{ij} + iIm\varepsilon_{ij})^2 - 1}{(Re\varepsilon_{ij} + iIm\varepsilon_{ij})^2 + 1}\right] \tag{5.6}$$

Optical absorption coefficient $A(\omega)$ is defined as follows in terms of real and imaginary parts of dielectric function:

$$A_{ij}(\omega) = \frac{\sqrt{2}\omega}{c}\left[(Re\varepsilon_{ij}^2 + Im\varepsilon_{ij}^2) - Re\varepsilon_{ij}\right]^{\frac{1}{2}} \tag{5.7}$$

Absorption is related to transition between occupied and unoc- cupied bands due to light and electron interaction. Optical conductivity is another quantity depending on the interband and intraband transitions. Optical conductivity is calculated in terms of $Im\varepsilon(\omega)$ as follows:

$$\delta_{ij}(\omega) = \frac{\omega_{ij}}{4\pi} Im\varepsilon_{ij}(\omega) \tag{5.8}$$

List of Abbreviations

BZ	:	Brillouin Zone
DFT	:	Density Functional Theory
DOS	:	Density of States
FLL	:	Fully Localized Limit
GGA	:	Generalized Gradient Approximation
HK	:	Hohenberg-Kohn
HM	:	Half-Metallic
KS	:	Kohn-Sham
LSDA	:	Local Spin Density Approximation
PDOS	:	Partial Density of States
PBE	:	Perdew Burke Ernzerhof
RMT	:	Radius Muffin Tin
RHF	:	Restricted Hartree Fock
XC	:	Exchange correlation

Bibliography

[1] PH Galanakis. Dederichs, and n. papanikolaou. Phys. Rev. B, 66(17):174429, 2002.

[2] Iosif Galanakis, Marjana Ležaić, Gustav Bihlmayer, and Stefan Blügel. Inter- face properties of NiMnSb/InP and NiMnSb/GaAs contacts. Phys. Rev. B, 71(21):214431, 2005.

[3] GY Gao, Lei Hu, KL Yao, Bo Luo, and Na Liu. Large half-metallic gaps in the quaternary heusler alloys CoFeCrZ (Z=Al, Si, Ga, Ge): A first-principles study. J. Alloys Compd, 551:539–543, 2013.

[4] GY Gao, Bin Xu, Zhi-Yuan Chen, and KL Yao. Surface d0 half-metallicity of rocksalt mgn from first-principles. J. Alloys Compd, 546:119– 123, 2013.

[5] RA De Groot, FM Mueller, PG Van Engen, and KHJ Buschow. New class of materials: half-metallic ferromagnets. Phys. Rev. Lett, 50(25):2024, 1983.

[6] Hideo Ohno. Making nonmagnetic semiconductors ferromagnetic. Science, 281(5379):951–956, 1998.

[7] Sabine Wurmehl, Gerhard H Fecher, Hem Chandra Kandpal, Vadim Kseno- fontov, Claudia Felser, and Hong-Ji Lin. Investigation of Co_2 Fe Si: The heusler compound with highest curie temperature and magnetic moment. Appl. Phys. Lett, 88(3):032503, 2006.

[8] Žutić, I., Fabian, J., & Sarma, S. D. (2004). Spintronics: Fundamentals and applications. Rev. Mod. Phys. 76(2), 323.

[9] Felser, C., Fecher, G. H., & Balke, B. (2007). Spintronics: a challenge for materials Science and solid-state chemistry. Angew. Chem. Int. Ed. 46(5), 668-699.

[10] Inomata, K., Ikeda, N., Tezuka, N., Goto, R., Sugimoto, S., Wojcik, M., & Jedryka, E. (2008). Highly spin-polarized materials and devices for spintronics. STAM, 9(1), 014101.

[11] De Groot, R. A., Mueller, F. M., van Engen, P. V., & Buschow, K. H. J. (1983). New class of materials: half-metallic ferromagnets. Phys. Rev. Lett, 50(25), 2024.

[12] Antoni Planes, Lluis Manosa, and Avadh Saxena. Magnetism and structure in functional materials. 1, 2005.

[13] I Galanakis, Ph Mavropoulos, and Ph H Dederichs. Electronic structure and slater–pauling behaviour in half-metallic heusler alloys calculated from first principles. J. Phys. D: Applied Physics, 39(5):765, 2006.

[14] Peter Entel, VD Buchelnikov, VV Khovailo, AT Zayak, WA Adeagbo, ME Gruner, HC Herper, and EF Wassermann. Modelling the phase diagram of magnetic shape memory heusler alloys. J. Phys D: Appl. Phys, 39(5):865, 2006.

[15] Antoni Planes, Lluis Manosa, and Mehmet Acet. Magnetocaloric effect and its relation to shape-memory properties in ferromagnetic heusler alloys. J. Phys: Condensed Matter, 21(23):233201, 2009.

[16] Markus E Gruner and Peter Entel. Impact of local lattice distortions on the structural stability of Fe-Pd magnetic shape-memory alloys. Phys. Rev. B, 83(21):214415, 2011.

[17] Peter Entel, Antje Dannenberg, Mario Siewert, Heike C Herper, Markus E Gruner, Vasiliy D Buchelnikov, and Volodymyr A Chernenko. Composition- dependent basics of smart heusler materials from first-principles calculations. 684:1–29, 2011.

[18] Tanja Graf, Claudia Felser, and Stuart SP Parkin. Simple rules for the understanding of heusler compounds. Progress in solid state chemistry, 39(1):1–50, 2011.

[19] Tomoyuki Kakeshita, Takashi Fukuda, Avadh Saxena, and Antoni Planes. Disorder and strain-induced complexity in functional materials, volume 148. SSBM, 2011.

[20] Peter Entel, Mario Siewert, Markus E Gruner, Heike C Herper, Denis Comtesse, Raymundo Arróyave, Navedeep Singh, Anjana Talapatra, Vladimir V Sokolovskiy, Vasiliy D Buchelnikov, et al. Complex magnetic ordering as a driving mechanism of multifunctional properties of heusler alloys from first principles. EPJ . B, 86(2):1–11, 2013.

[21] Peter Entel, Antje Dannenberg, Mario Siewert, Heike C Herper, Markus E Gruner, Denis Comtesse, Hans-Joachim Elmers, and Michael Kallmayer. Basic properties of magnetic shape-memory materials from first-principles calculations. Metallurgical and Materials Transactions A, 43(8):2891–2900, 2012.

[22] KA Kilian and RH Victora. Electronic structure of Ni_2MnIn for use in spin injection. J. Appl. Phys. 87(9):7064–7066, 2000.

[23] JMD Coey, M Venkatesan, and MA Bari. ed c bertheir et al, 2002.

[24] KA Kilian and RH Victora. Electronic structure of Ni_2MnIn for use in spin injection. J. Appl. Phys. 87(9):7064–7066, 2000.

[25] Friedrich Heusler. Über magnetische manganlegierungen. Verh. Dtsch. Phys. Ges, 5(12):219, 1903.

[26] Kervan, N., & Kervan, S. (2012). Half-metallicity in the full-Heusler Fe_2MnP compound. Intermetallics, 24, 56-59.

[27] Gary A Prinz. Magnetoelectronics. Science, 282(5394):1660–1663, 1998.

[28] Birsan, A., and V. Kuncser. Theoretical investigations of electronic structure and magnetism in Zr_2CoSn full-Heusler compound. J. Magn. Mater 388 (2015): 1-4..

[29] Capelle, K. (2006). A bird's-eye view of density-functional theory. Braz. J. Phys, 36, 1318-1343.

[30] Koch, W., & Holthausen, M. C. (2015). A chemist's guide to density functional theory. John Wiley & Sons.

[31] Gupta, Vijay P. Principles and applications of quantum chemistry. Academic Press, 2015.

[32] Parr, Robert G. Density functional theory of atoms and molecules. Horizons of quantum chemistry. Springer, Dordrecht, 1980. 5-15.

[33] Schrödinger, Erwin. An undulatory theory of the mechanics of atoms and molecules. Phys. Rev. 28.6 (1926): 1049.

[34] F Schwabl. Quantum mechanics (qm i). ; quantenmechanik (qm i). eine ein- fuehrung. 2007.

[35] Arthur Jabs. Connecting spin and statistics in quantum mechanics. Foundations of Physics, 40(7):776–792, 2010.

[36] Pierre Hohenberg and Walter Kohn. Inhomogeneous electron gas. Phys. Rev , 136(3B):B864, 1964.

[37] DJ Griffiths. Introduction to quantum mechanics 2nd ed.-solutions. 2005.

[38] Max Born. Quantenmechanik der stoßvorgänge. Zeitschrift für physik, 38(11):803–827, 1926.

[39] David C Young. Density functional theory. Computational Chemistry, pages 42–48, 2001.

[40] Arthur Jabs. Connecting spin and statistics in quantum mechanics. Foundations of Physics, 40(7):776–792, 2010.

[41] Wolfgang Pauli. The connection between spin and statistics. Phys. Rev, 58(8):716, 1940.

[42] Pauli, W. (1925). On the connexion between the completion of electron groups in an atom with the complex structure of spectra. Zeitschrift für Physik, 31, 765.

[43] Nouredine Zettili. Quantum mechanics: concepts and applications, 2003.

[44] Klaus Capelle. A bird's-eye view of density-functional theory. Braz. J. Phys. 36:1318–1343, 2006.

[45] Tatu Ra janiemi. Electronic and optical properties of TiO_2 nanoclus- ters. Am. J. Phys. 2016.

[46] David C Young. Density functional theory. Computational Chemistry, pages 42–48, 2001.

[47] Niklas Zwettler. Density functional theory.

[48] F Schwabl. Quantum mechanics (qm i). ; quantenmechanik (qm i). eine ein- fuehrung. 2007.

[49] DJ Griffiths. Introduction to quantum mechanics 2nd ed.-solutions. 2005.

[50] Paul Adrien Maurice Dirac. A new notation for quantum mechanics. In Mathematical Proceedings of the Cambridge Philosophical Society, volume 35, pages 416–418. Cambridge University Press, 1939.

[51] Lang, Christian B., and Norbert Pucker. Mathematische methoden in der physik. Vol. 2. Springer Spektrum, 2005.

[52] Wolfgang Pauli. The connection between spin and statistics. Phys. Rev, 58(8):716, 1940.

[53] Szabo, A., & Ostlund, N. S. (1989). Modern Quantum Chemistry, revised 1st edition.

[54] Pavarini, Eva, Erik Koch, and Ulrich Schollwöck, eds. Emergent Phenomena in Correlated Matter: Autumn School Organized by the Forschungszentrum Jülich and the German Research School for Simulation Sciences at Forschungszentrum Jülich 23-27 September 2013; Lecture Notes of the Autumn School Correlated Electrons 2013. Vol. 3. Forschungszentrum Jülich, 2013.

[55] F Schwabl. Quantum mechanics (qm i). ; quantenmechanik (qm i). eine ein- fuehrung. 2007.

[56] Leifhelm, Alexander. Die Legendre-Transformation als geometrisches Mittel der Variablentransformation in der Physik. (2015).

[57] Wolfgang Pauli. The connection between spin and statistics. Phys. Rev, 58(8):716, 1940.

[58] Walter Kohn. Nobel lecture: Electronic structure of matter—wave functions and density functionals. Rev. Mod. Phys . 71(5):1253, 1999.

[59] Walter Kohn. Nobel lecture: Electronic structure of matter—wave functions and density functionals. Rev. Mod. Phys . 71(5):1253, 1999.

[60] Harrison, N. M. (2003). An introduction to density functional theory. Nato Science Series Sub Series III Computer and Systems Sciences, 187, 45-70.

[61] Jensen, Frank. Introduction to computational chemistry. John wiley and sons, 2017.

[62] Yin, Zhiping. Microscopic mechanisms of magnetism and superconductivity studied from first principle calculations. University of California, Davis, 2009.

[63] Felix Brockherde, Leslie Vogt, Li Li, Mark E Tuckerman, Kieron Burke, and Klaus-Robert Müller. Bypassing the kohn-sham equations with machine learning. Nature communications, 8(1):1–10, 2017.

[64] Tsegaye, Zenebe Assefa. Density functional theory studies of electronic and optical properties of ZnS alloyed with Mn and Cr. MS thesis. Institutt for fysikk, 2012.

[65] Tatu Ra janiemi. Electronic and optical properties of TiO_2 nanoclus- ters. Am. J. Phys. 2016.

[66] Lewars, E. (2011). Computational chemistry. Introduction to the theory and applications of molecular and quantum mechanics, 318.

[67] Nathan Argaman and Guy Makov. Density functional theory-an introduction. Am. J. Phys. 1998.

[68] Karlheinz Schwarz. DFT calculations of solids with LAPW and WIEN2k. J. Solid State Chem . 176:319–328, 2003.

[69] Perdew, J. P., Burke, K., & Ernzerhof, M. (1996). Generalized gradient approximation made simple. Phys. Rev. Lett, 77(18), 3865.

[70] Perdew, J. P., Burke, K., & Wang, Y. (1996). Generalized gradient approximation for the exchange-correlation hole of a many-electron system. Phys. Rev. B, 54(23), 16533.

[71] Balàzs, N. L. (1967). Formation of stable molecules within the statistical theory of atoms. Phys. Rev, 156(1), 42.

[72] Isyaku, Abdullahi Odoguje. Structural, Electronic and Optical Properties of Cu_2Sns_3 Solar Absorber: A First-Principle Density Functional Theory Investigation. Diss. 2019.

[73] Wang, J., Wang, Z., Jing, Y., Wang, S., Chou, C. F., Hu, H., ... & Su, W. S. (2016). Electronic structure and optical properties of boron suboxide B_6O system: First-principles investigations. Solid State Communications, 244, 12-16.